

Microporous organic polymers incorporating dicarboximide units for H₂ storage and remarkable CO₂ capture

Saad Makhseed^a* and Jacob Samuel^b

^aChemistry Department, Kuwait University, Safat, Kuwait. E-mail: saad.makhseed@ku.edu.kw; Fax: +965 2481 6482; Tel: +965 24985538

^bThe Petroleum Research Center, Kuwait Institute for Scientific Research, Ahmadi, Kuwait

Supporting information

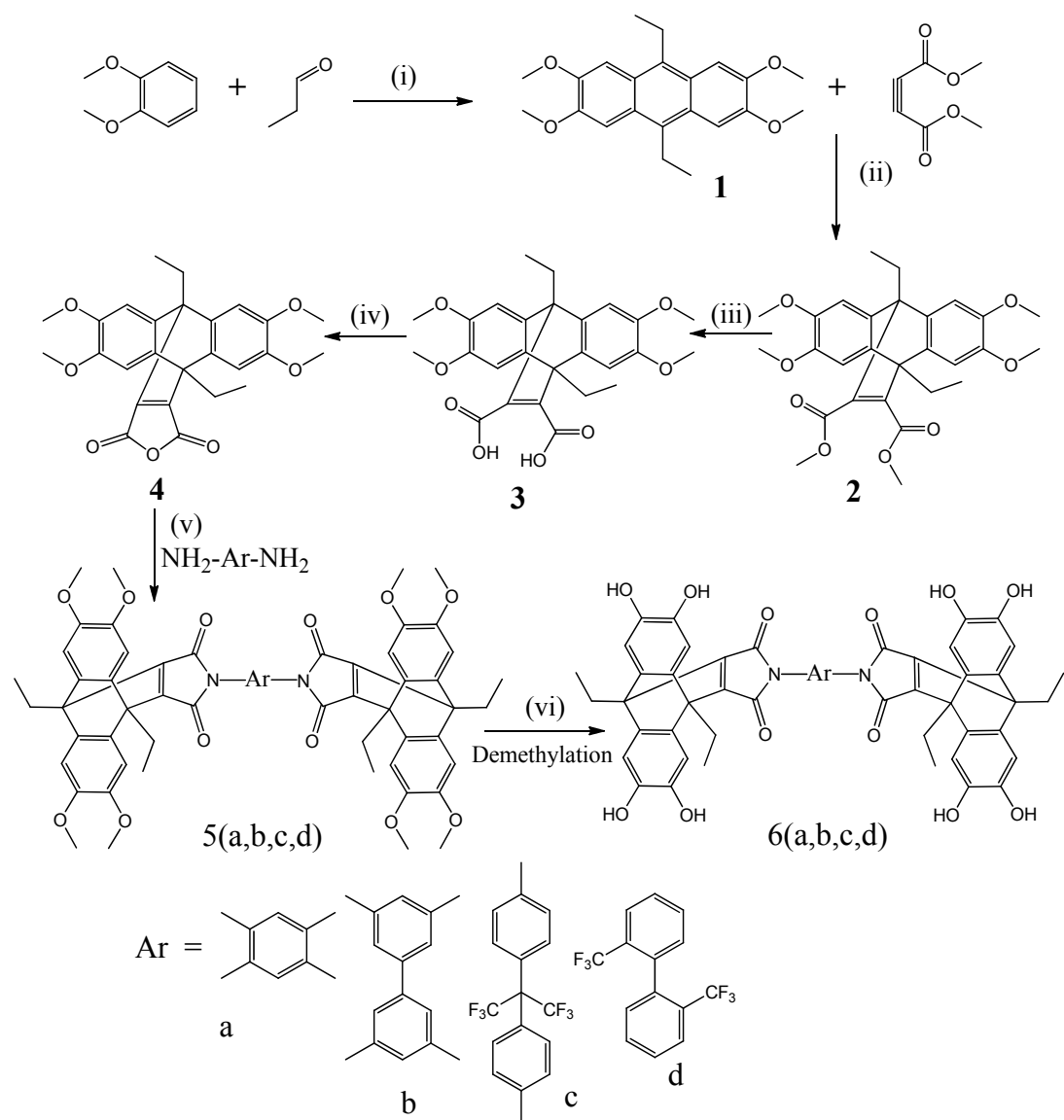
Table of content:

Scheme of preparation of monomers, FTIR, ¹H NMR spectra of monomers; FTIR, and solid state ¹³CNMR spectra of polymers, XPS analysis, HRTEM analysis, TGA of polymers, porous properties of Polymers (linear plot, BET plots, NLDFT and HK plots); H₂ and CO₂ adsorption isotherms.

1. Experimental

1.1 Materials

Following outlined pathway has been used to prepare the octahydroxy monomers with different spacers.



Scheme S1. Synthetic pathway towards the octahydroxy monomers. Reagents and conditions: (i) 84% sulfuric acid, 0–5°C; (ii) 220°C, 20 minutes; (iii) ethanol-water, (1:1 volume) reflux, 3 h; (iv) acetic anhydride, reflux, 3 h; (v) Acetic acid, reflux, 24 h; (vi) BBr_3 , CH_2Cl_2 , 0–5 °C, 3 h;

1.2.1 Synthesis of 9,10-diethyl-2,3,6,7-tetramethoxyanthracene [1]

To a solution of veratrole (13.75 g, 99.13 mmol) and propanal (28.75 g, 495 mmol) in chloroform (50 ml), 84% sulfuric acid (100 ml) was added dropwise while the temperature was kept between 0 and 5 °C. Then stirred for 6 hrs at room temperature. On cooling the reaction mixture was neutralized with aqueous ammonia. The resulting precipitate was collected by filtration and washed several times with water and methanol. The crude product was crystallized from methanol to afford **1** as a white powder. Yield 62 %; m.p. 245 °C; MS (EI): m/z 354 (M^+). 1H NMR ($CDCl_3$, 400 MHz, δ ppm): 1.46 (t, 12H), 3.48 (q, 4H) 4.09 (s, 12H), and 7.43 (s, 4H). IR/cm⁻¹ (KBr): 1225 (C-O), CHN calculated for $C_{22}H_{30}O_4$ (358): C, 73.56; H, 8.22; found C, 73.71; H, 8.44.

1.2.2 Synthesis of dimethyl9,10-diethyl-2,3,6,7-tetramethoxy-9,10-dihydro-9,10-ethenoanthracene-11,12-dicarboxylate [2]

A mixture of **1** (4.00 g, 11.29 mmol) and dimethylacetylenedicarboxylate (10 ml) was heated in bulk at 220 °C for 20 min. The resultant solid product was recrystallized from 1,4-dioxane followed by refluxing in methanol to afford **2** as pale brown powder in 90 % yield; m.p. 243 °C; MS (EI): m/z 496 (M^+). 1H NMR ($DMSO-d_6$, 400 MHz, δ ppm): 1.25-1.31 (t, 6H), 2.85-2.87 (m, 4H), 3.70 (d, 6H), 3.83 (s, 12H) and 6.91 (s, 4H). IR/cm⁻¹ (KBr): 1780 (asym C=O, str), 1725 (sym C=O, str). CHN Calculated for $C_{28}H_{32}O_8$ (496): C, 67.73; H, 6.50. Found: C, 67.48; H, 7.02.

1.2.3 Synthesis of 9,10-diethyl-2,3,6,7-tetramethoxy-9,10-dihydro-9,10-ethenoanthracene-11,12-dicarboxylic acid [3]

To a solution of ethanol/water (1:1 volume; 280 ml), potassium hydroxide (10.00 g, 20.16 ml) was added slowly followed by **2** (10.00 g, 178.57 mmol). The reaction mixture was refluxed with stirring for 3 h, and the resulting solution was hot-filtered to remove any insoluble particles. After cooling, the filtrate was acidified. The resulting white precipitate was filtered off, washed with water followed by hexane, and dried to yield the derivative in 95% as a white solid which was used in the next reaction without any further purification. m.p. 215 °C; MS (EI): m/z 496 (M^+); 1H NMR ($DMSO-d_6$, 400 MHz, δ ppm): 1.31 (t, 6H), 2.8 (q, 4H), 3.73 (s, 12H), 6.9 (s, 4H), and 13.04 (s, 2H). IR/cm⁻¹ (KBr): 3373 (OH), 3017 (aromatic C-H), 2945 (aliphatic C-H), 1715 (C=O), 1216 (C-O-C str). CHN Calculated for $C_{28}H_{32}O_8$ (496): C, 67.73; H, 6.50. Found: C, 67.54; H, 6.28.

1.2.4. Synthesis of 9,10-diethyl-2,3,6,7-tetramethoxy-9,10-[3,4]furanoanthracene-12,14(9H,10H)-dione [4]

The solid of **3** (5.00 g, 11.11 mmol) was added to acetic anhydride (200 ml). The resulting mixture was heated under reflux and nitrogen atmosphere for 4 h. On cooling, the pale brown was collected by filtration, washed with acetic acid and toluene, then dried at 80 °C under vacuum to give 4 in 66 %; m.p. 216 °C; MS (EI): m/z 450 (M^+). 1H NMR (CDCl₃, 400 MHz, δ ppm): 1.68 (t, 6H), 2.86 (q, 4H), 3.87 (s, 12H) and 6.97 (s, 4H). IR/cm⁻¹ (KBr): 2938, 1835, 1762, 1418, 1267, 1047, 898. CHN Calculated for C₂₆H₂₆O₇ (450): C, 69.32; H, 5.82. Found: C, 69.18; H, 5.87.

1.3.1 Synthesis of octamethoxy-anthracene based precursor [5a]

The anhydride **4** (5.00 g, 11.11 mmol) was added to a stirred solution of 2,3,5,6-tetramethyl-1,4-phenylenediamine (0.86 g, 5.29 mmol) in glacial acetic acid and refluxed for 12 h. The obtained white solid was further refluxed in acetic anhydride for another 12 h. After cooling, the precipitated product was filtered off and washed with petroleum ether to give a light yellow solid. Yield 70%; m.p. > 300 °C; MS (EI) m/z: 1028 (M^+). 1H NMR (DMSO-d₆, 400 MHz, δ ppm): 1.55 (t, 12H), 1.78 (s, 12H), 2.83 (m, 8H), 3.75 (s, 24H) and 7.03 (s, 8H). IR/cm⁻¹ (KBr): 2937, 1764, 1710, 1486, 1344, 1049, 765. CHN Calculated for C₆₂H₆₄N₂O₁₂: C, 72.36; H, 6.27; N, 2.72. Found: C, 72.68; H, 6.21; N, 2.63.

The following octamethoxy-anthracene based units were prepared from the anhydride derivative (4) and different aromatic diamines spacers using similar procedure adopted for 5a.

1.3.2 Synthesis of octamethoxy-anthracene based precursor [5b]

Yield 70%; m.p. > 300 °C; MS (EI) m/z: 1104 (M^+). 1H NMR (DMSO-d₆, 400 MHz, δ ppm): 1.57 (t, 12H), 1.96 (s, 12H), 2.86 (m, 8H), 3.76 (s, 24H) 7.04 (s, 8H) and 7.48 (s, 4H). IR/cm⁻¹ (KBr): 2938, 1764, 1710, 1481, 1365, 1272, 1049. CHN Calculated for C₆₈H₆₈N₂O₁₂: C, 73.89; H, 6.20; N, 2.53. Found: C, 74.24; H, 6.38; N, 2.31.

1.3.4 Synthesis of octamethoxy-anthracene based precursor [5c]

Yield 85%; m.p. > 300 °C. MS (EI) m/z: 1225 (M^+). 1H NMR (DMSO-d₆, 400 MHz, δ ppm): 1.55 (t, 12H), 1.97 (S, 6H), 2.81(q, 8H), 3.75 (s, 24H). 6.99 (d, 4H), 7.16 (d, 2H), 7.31 (s, 2H), 7.41 (d, 4H). IR/cm⁻¹ (KBr): 2938, 1768, 1712, 1486, 1371, 1253. CHN Calculated for C₆₉H₆₄F₆N₂O₁₂: C, 67.53; H, 5.26; N, 2.28. Found: C, 67.54; H, 5.33; N, 2.56.

1.3.3 Synthesis of octamethoxy-anthracene based precursor [5d]

Yield 82 %; m.p. > 300 °C; MS (EI) m/z: 1185 (M^+). 1H NMR (DMSO-d₆, 400 MHz, δ ppm): 1.60 (t, 12H), 2.86(q, 8H), 3.75 (s, 24H). 7.04 (s, 8H), 7.50 (d, 2H), 7.66 (d, 2H), 7.89 (s, 2H), IR/cm⁻¹ (KBr):

2937, 1770, 1712, 1484, 1253, 751. CHN Calculated for C₆₆H₅₈F₆N₂O₁₂ (1185): C, 66.89; H, 4.93; N, 2.36. Found: C, 66.78; H, 4.72; N, 2.33.

1.4.1 Synthesis of octahydroxy monomer [6a]

To a stirred solution of **5a** (6.3 g, 10 mmol) in dry dichloromethane (300 ml) kept at 0 °C borontribromide diluted in dichloromethane (5.7 ml, 60 mmol) was added slowly. After the complete addition of borontribromide, the ice bath was removed and the reaction mixture further stirred for 3 hrs at room temperature. The reaction mixture was then poured onto ice and the organic layer was collected and evaporated under reduced pressure. The crude product was purified by column chromatography (eluent: 1: 4 methanol/chloroform) to afford **6a** as pale brown powder. Yield 88 %; MS (EI): m/z 916 (M⁺). ¹H NMR (DMSO-D₆, 400 MHz, δ ppm): 1.48 (t, 12H), 1.76 (s, 12H), 2.59 (m, 8H), 6.76 (s, 8H) and 8.80 (s, 8H). IR/cm⁻¹(KBr): 3450, 2938, 1762, 1706, 1614, 1481, 1299, 792. CHN Calculated for C₅₄H₄₈N₂O₁₂: C, 70.73; H, 5.28; N, 3.05. Found: C, 70.34; H, 5.08; N, 2.98.

The following octahydroxy monomers were prepared from corresponding methoxy precursors using similar procedure adopted for 5a.

1.4.2 Synthesis of monomer [6b]

Yield 88%; MS (EI) m/z: 993 (M⁺). ¹H NMR (DMSO-D₆, 400 MHz, δ ppm): 1.50 (t, 12H), 1.95 (s, 12H), 2.61 (m, 8H), 6.80 (s, 8H) and 7.53 (s, 4H), 8.77 (s, 8H). IR/cm⁻¹ (KBr): 3428, 2929, 1764, 1704, 1448, 796. CHN Calculated for C₇₂H₅₂N₂O₁₂: C, 72.57; H, 5.28; N, 2.82. Found: C, 71.34; H, 5.16; N, 2.94.

1.4.3 Synthesis of monomer [6c]

Yield 88%; MS (EI) m/z: 1116 (M⁺). ¹H NMR (DMSO-d₆, 400 MHz, δ ppm): 1.48 (t, 12H), 1.98 (s, 6H), 2.56 (m, 8H), 6.78 (d, 8H), 7.14 (d, 2H), 7.28 (s, 2H), 7.41 (d, 2H), 8.74 (br s, 8H), IR/cm⁻¹ (KBr): 3427, 2927, 1773, 1704, 1449, 1296, 787. CHN Calculated for C₆₁H₄₈F₆N₂O₁₂ (1116): C, 65.71; H, 4.34; N, 2.51. Found: C, 66.18; H, 4.68; N, 2.41.

1.4.4 Synthesis of monomer [6d]

Yield 88%; MS (EI): m/z 1028 (M⁺ - 44). ¹H NMR (DMSO-d₆, 400 MHz, δ ppm): 1.42 (t, 12H), 2.59(m, 8H), 6.79 (d, 8H), 7.14 (d, 2H), 7.15 (s, 2H), 7.42 (d, 2H), 8.74 (br s, 8H). IR/cm⁻¹ (KBr): 3438, 2943, 1776, 1721, 1664, 1491, 784. CHN Calculated for C₅₈H₄₂F₆N₂O₁₂: C, 64.93; H, 3.95; N, 2.61. Found: C, 64.58; H, 3.76; N, 2.54.

The synthesis of microporous polymers (AMPs) was carried out by the polycondensation of the octa-functional monomers containing different spacers in dry DMF using anhydrous potassium carbonate as a base (Scheme 2).

2. Synthesis of AMPs

2.1 Synthesis of AMP-1

To a solution of **6a** (0.2 g, 0.21 mmol) and 2,3,5,6-tetrafluorophalonitrile (0.08 g, 0.43 mmol) in dry DMF (40 ml), K₂CO₃ (0.35 g, 2.52 mmol) was added and heated to 120 °C for 24 h. Then the reaction mixture was allowed to cool and precipitated in acidified water. The precipitate was filtered off and washed with deionised water and then with methanol. The purification was done by refluxing the crude product with deionised water, THF, methanol and acetone respectively to yield a brown powder. Yield 85 %. m.p.> 300 °C IR/cm⁻¹ (KBr): 2965, 2242, 1776, 1717, 1632, 1445, 1269, 1008. ¹³C NMR (150 MHz): 197.75, 172.36, 164.55, 137.7, 136.57, 131.40, 110.62, 64. 84, 61.10, 52.11, 45.78, 19.1, 13.22, 8.22. CHN Calculated for C₇₁H₅₂N₆O₁₂: C, 72.19; H, 4.44; N, 7.11. Found: C, 71.68; H, 3.89, N, 7.56.

The following AMPs were prepared from corresponding monomers using similar procedure adopted for AMP-1

2.2 Synthesis of AMP-2

Yield 85%; m.p.> 300 °C; IR/cm⁻¹ (KBr): 2928, 2242, 1771, 1716, 1666, 1441, 1269, 1008. ¹³C NMR (150 MHz): 169.8, 147.5, 146.3, 142.8, 141.8, 137.9, 137.6, 134.5, 125.4, 115.8, 105.6, 42.9, 39.6, 18.1, 10.3, 9.0, 8.5. CHN Calculated for C₇₆H₅₂N₆O₁₂: C, 73.54; H, 4.22; N, 6.77. Found: C, 71.88; H, 4.03, N, 7.26.

2.3 Synthesis of AMP-3

Yield 85%; m.p.> 300 °C; IR/cm⁻¹ (KBr): 2954, 2239, 1773, 1721, 1460, 1314, 984. ¹³C NMR (150 MHz): 183.94, 156.00, 146.62, 139.24, 129.63, 109.69, 86.44, 56.28, 41.88, 28.97, 15.98. CHN Calculated for C₇₇H₄₈F₆N₆O₁₂: C 67.84; H, 3.55; N, 6.16. Found: C, 67.70; H, 4.21, N, 7.22.

2.4 Synthesis of AMP-4

Yield 85%; m.p.> 300 °C; IR/cm⁻¹ (KBr): 2927, 2238, 1771, 1717, 1445, 1270, 1012. ¹³C NMR (150 MHz): 156.99, 141.91, 134.56, 119.81, 105.09, 51.55, 37.09 23.89. CHN Calculated for C₇₄H₄₂F₆N₆O₁₂: C, 67.27; H, 3.20; N, 6.36. Found: C, 67.28; H, 3.37, N, 7.65.

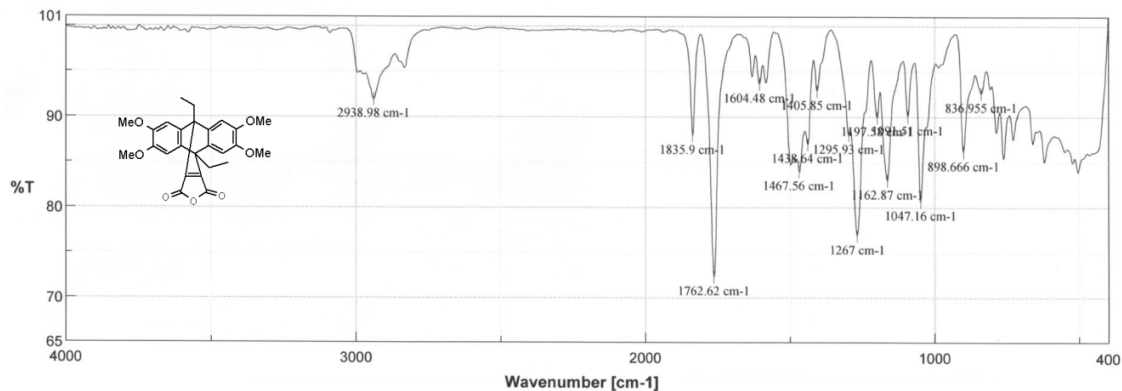


Figure S1a: FTIR Spectrum of anhydride: The characteristic bands related to the anhydride are 1762 and 1835 (C=O symmetric and asymmetric)

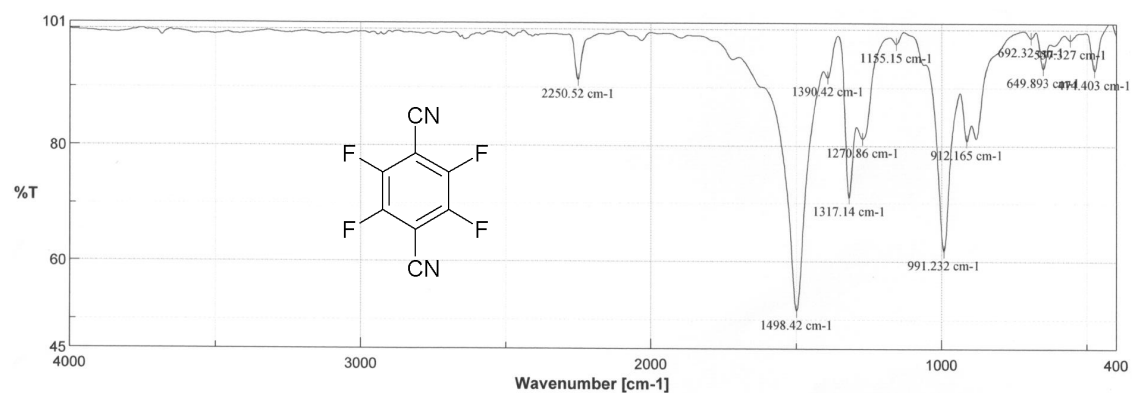


Figure S1b: FTIR Spectrum of tetrafluoroterephthalonitrile: The FTIR spectrum of tetrafluoroterephthalonitrile show a peak around 2250 (characteristic of nitrile group)

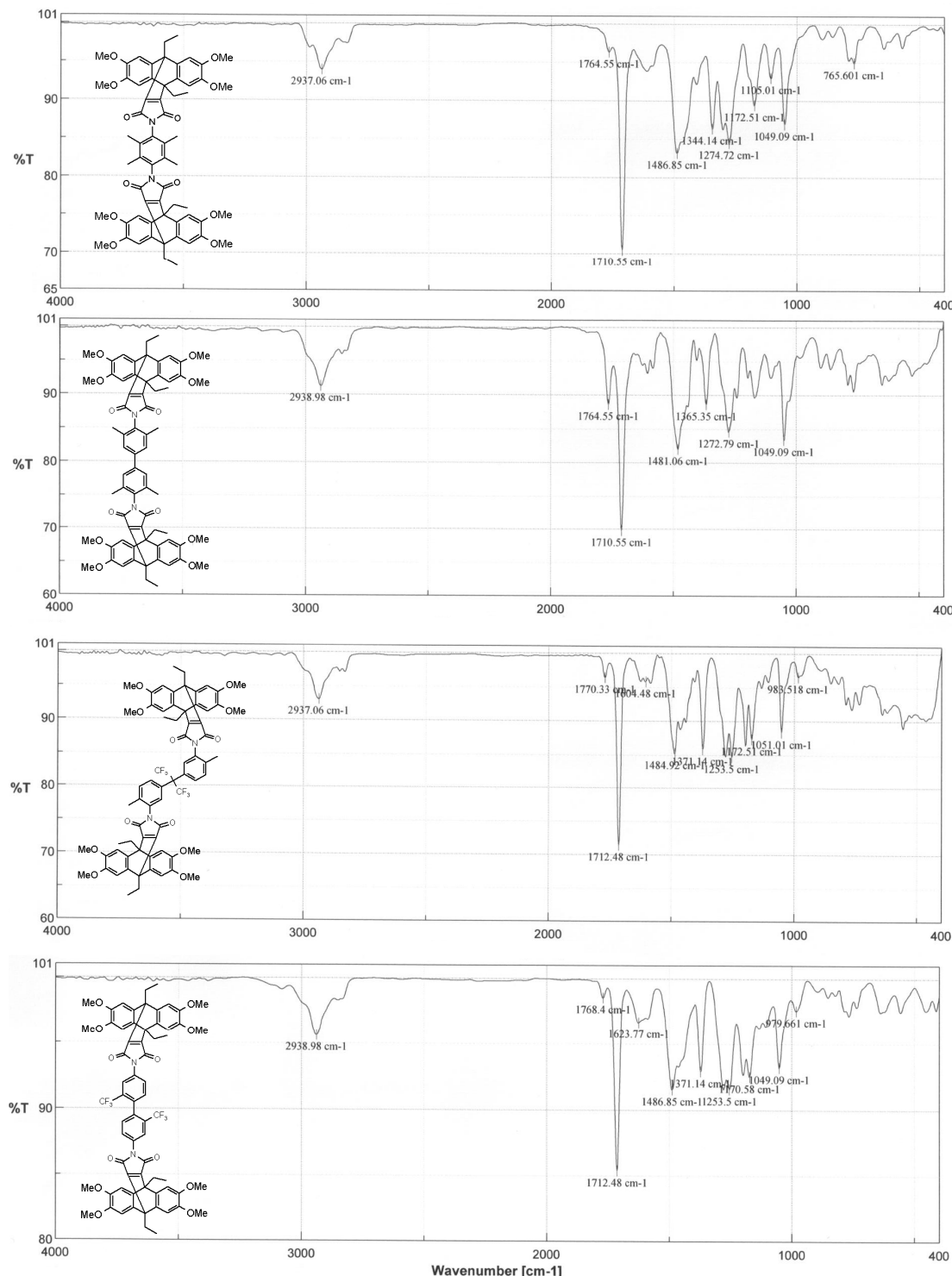


Figure S1c: FTIR Spectrum of octamethoxybismalimides. As shown in all figures, the characteristic bands related to the imide stretching (C=O symmetric and asymmetric bands in the range of 1722-1792) found in the spectrum of all the 4 molecules. Another feature is the presence of strong bands observed at 1481 characteristics of aromatic C=C bond.

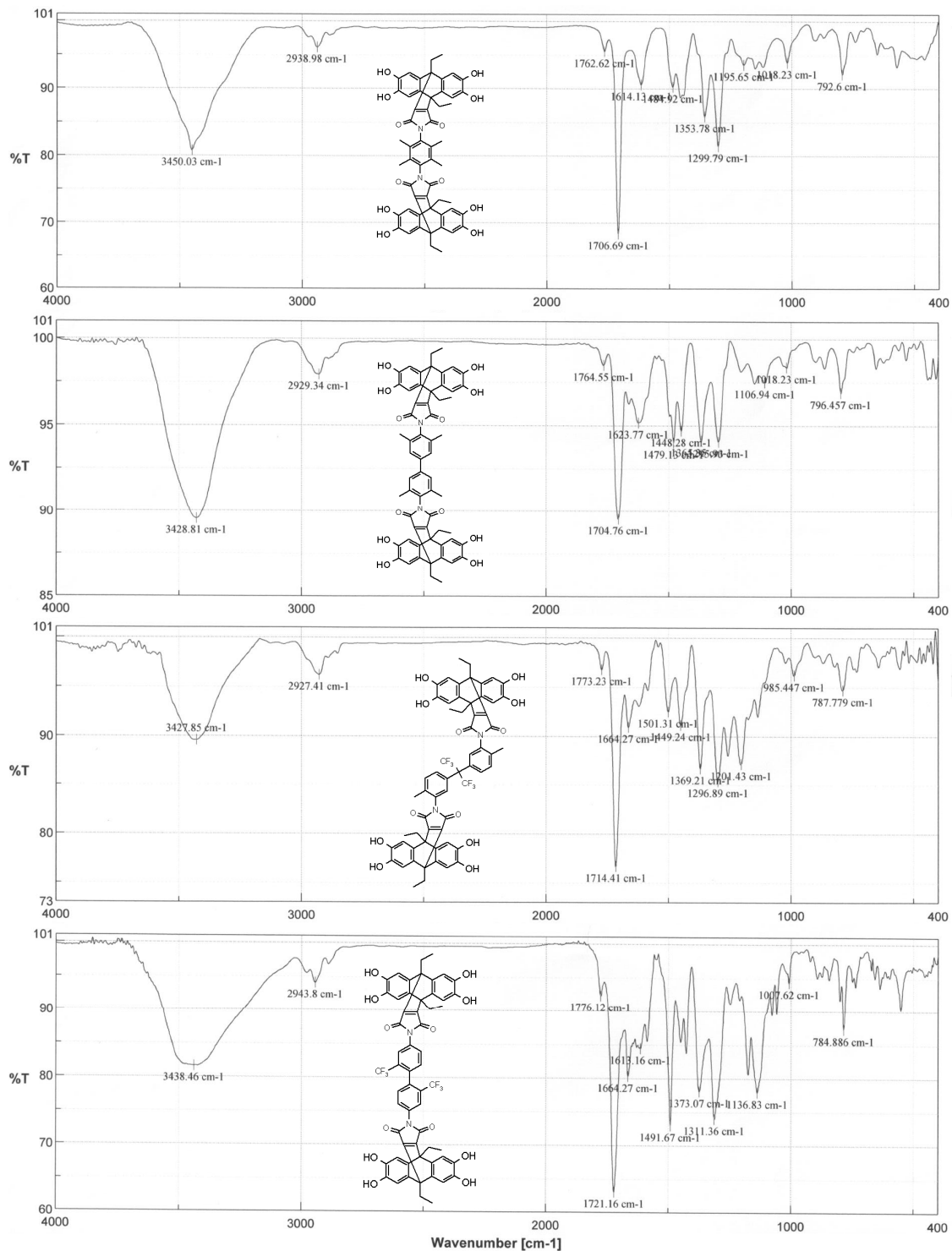


Figure S1d: FTIR Spectrum of octahydroxy monomers: The FTIR spectrum of each compound verifying its structure. A broad band around 3427-3428 is identified as hydroxyl groups. The two bands at 1700 and 1770 are characteristic of imide group.

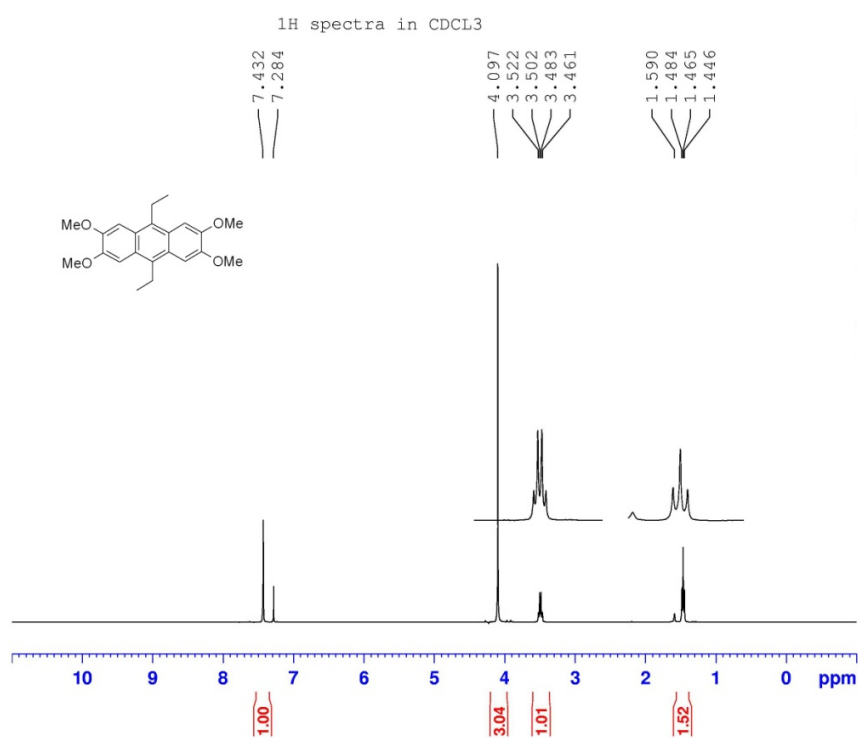


Figure S2a. ¹H NMR Spectrum of precursor molecule (1)

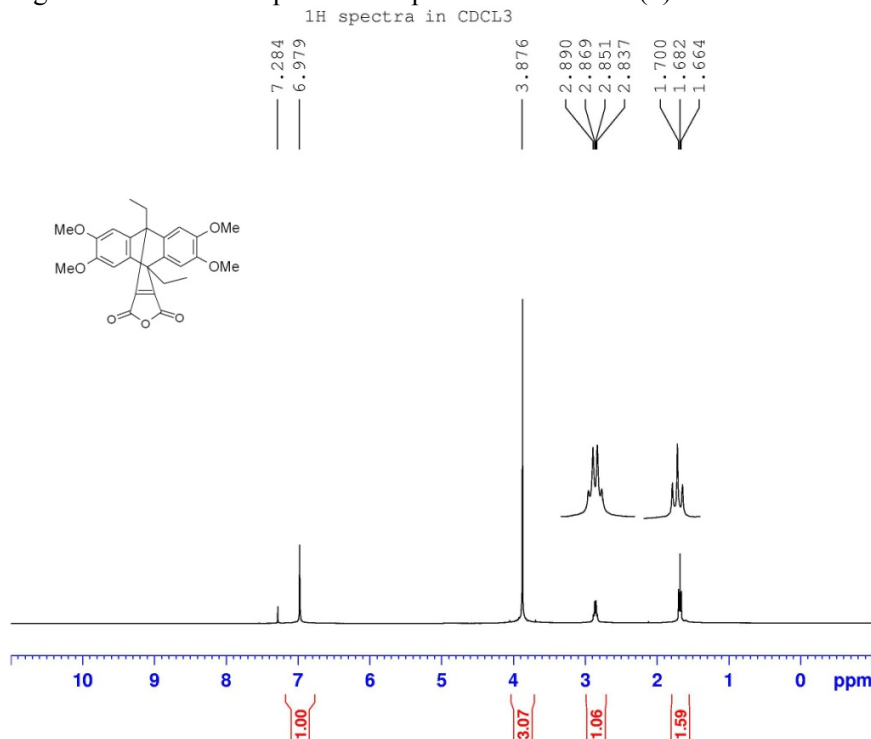


Figure S2b: ¹H NMR Spectrum of compound 4

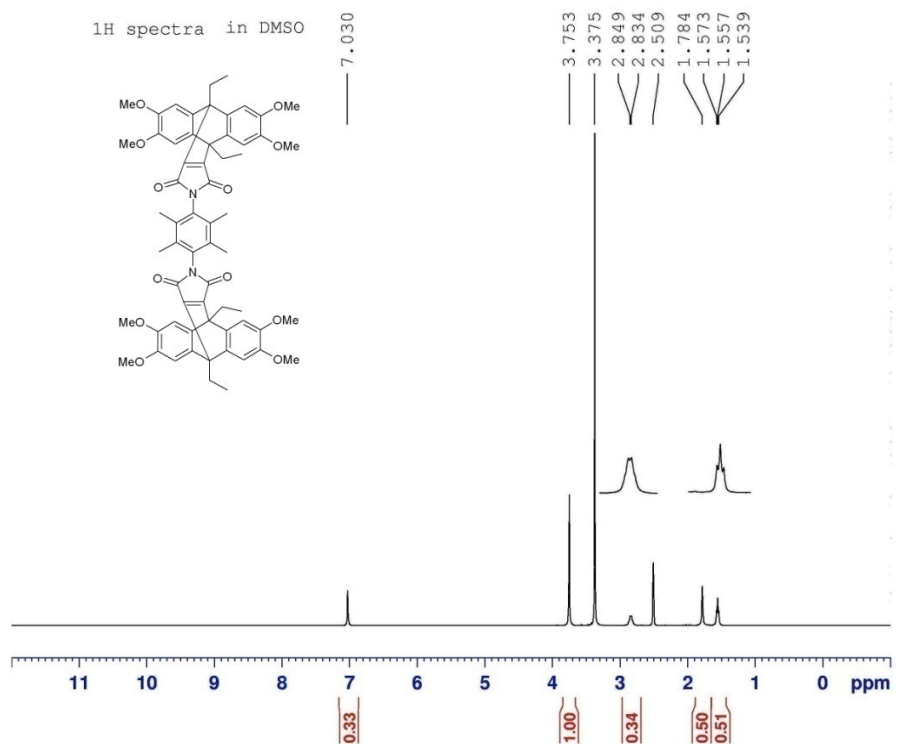


Figure S2c: ^1H NMR Spectrum of 5a

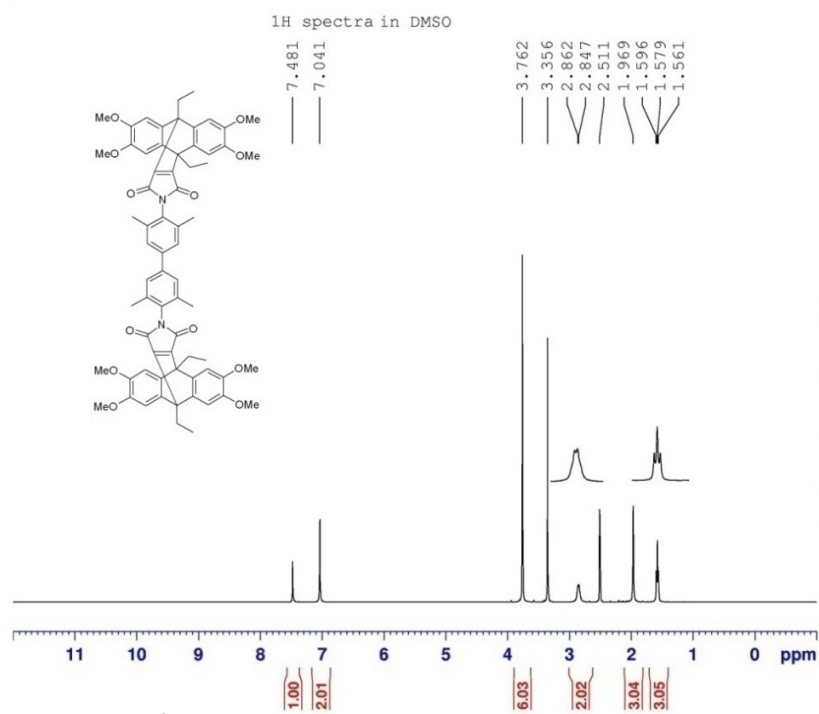


Figure S2d: ^1H NMR Spectrum of 5b

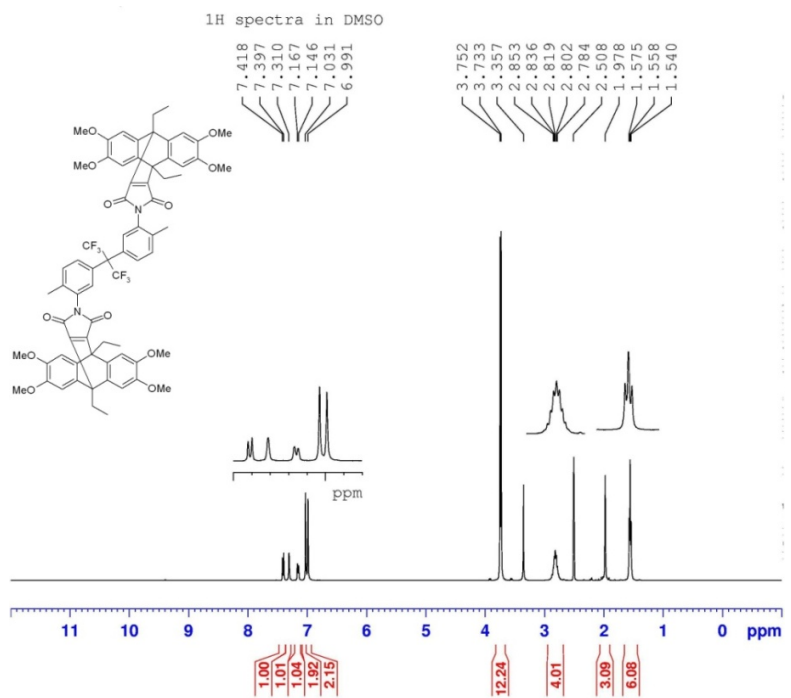


Figure S2e: ^1H NMR Spectrum of 5c

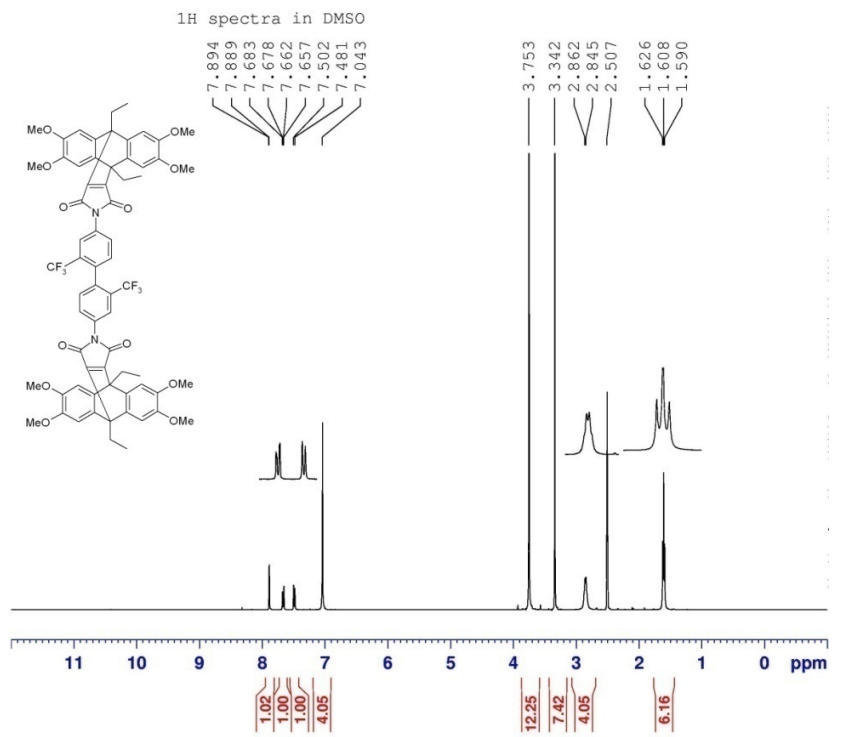


Figure S2f: ^1H NMR Spectrum of 5d

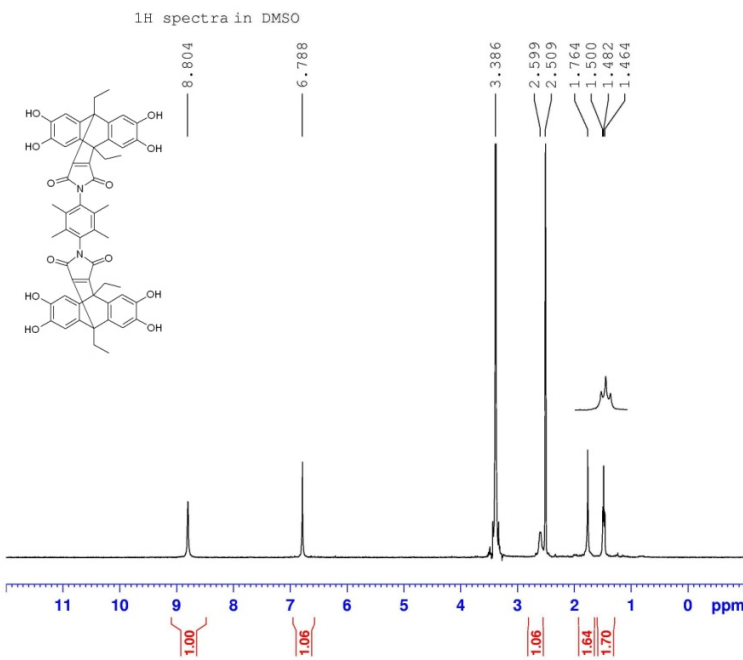


Figure S2g: ¹H NMR Spectrum of 6a

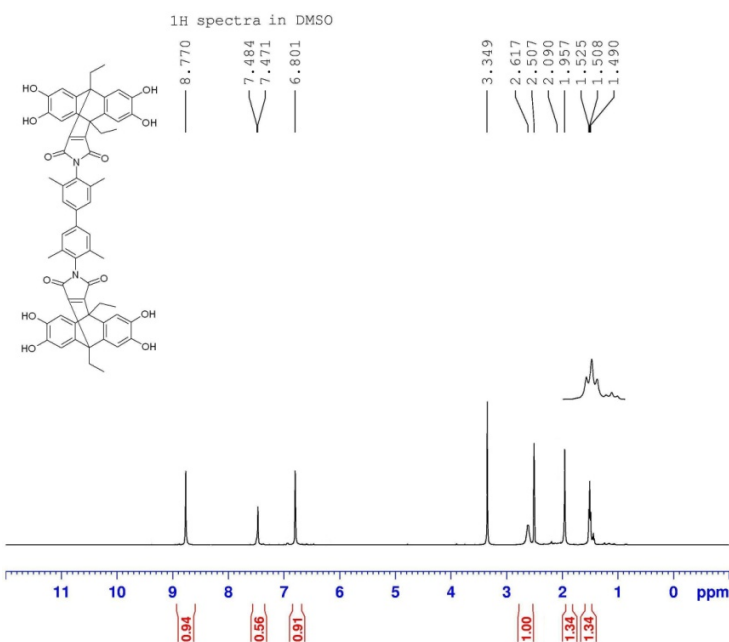


Figure S2h: ¹H NMR Spectrum of 6c

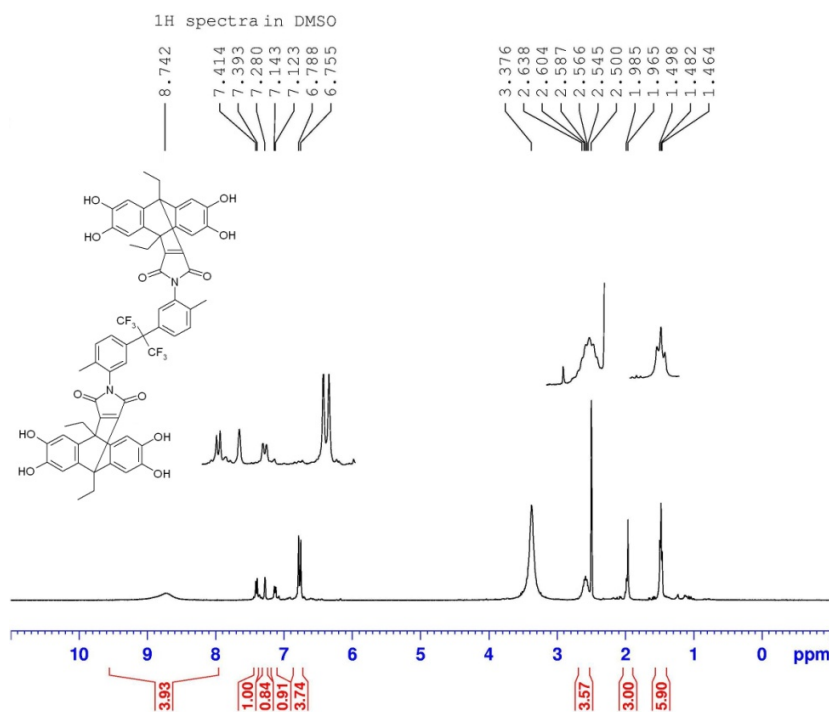


Figure S2i: ^1H NMR Spectrum of 6d

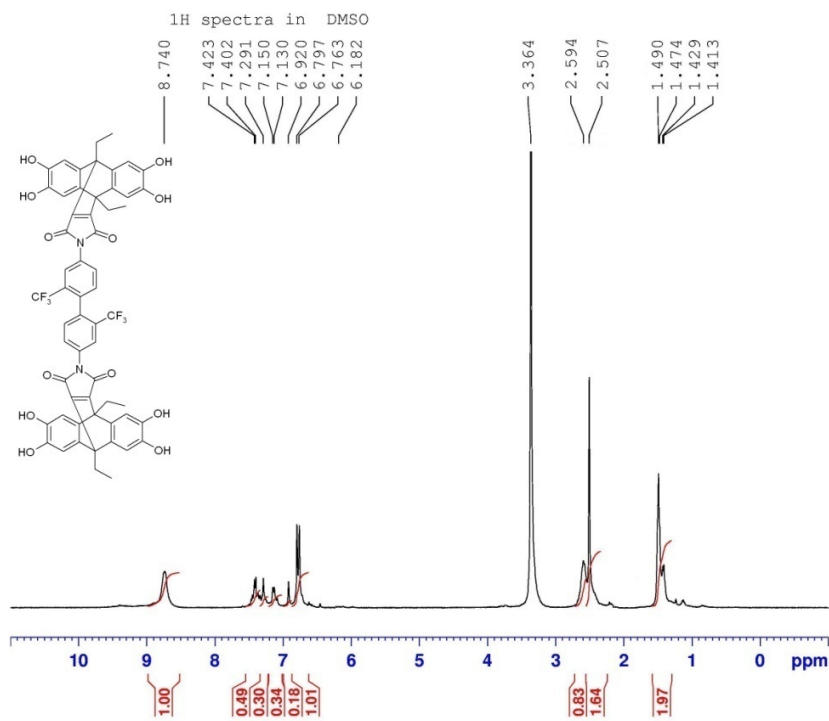


Figure S2j: ^1H NMR Spectrum of 6e

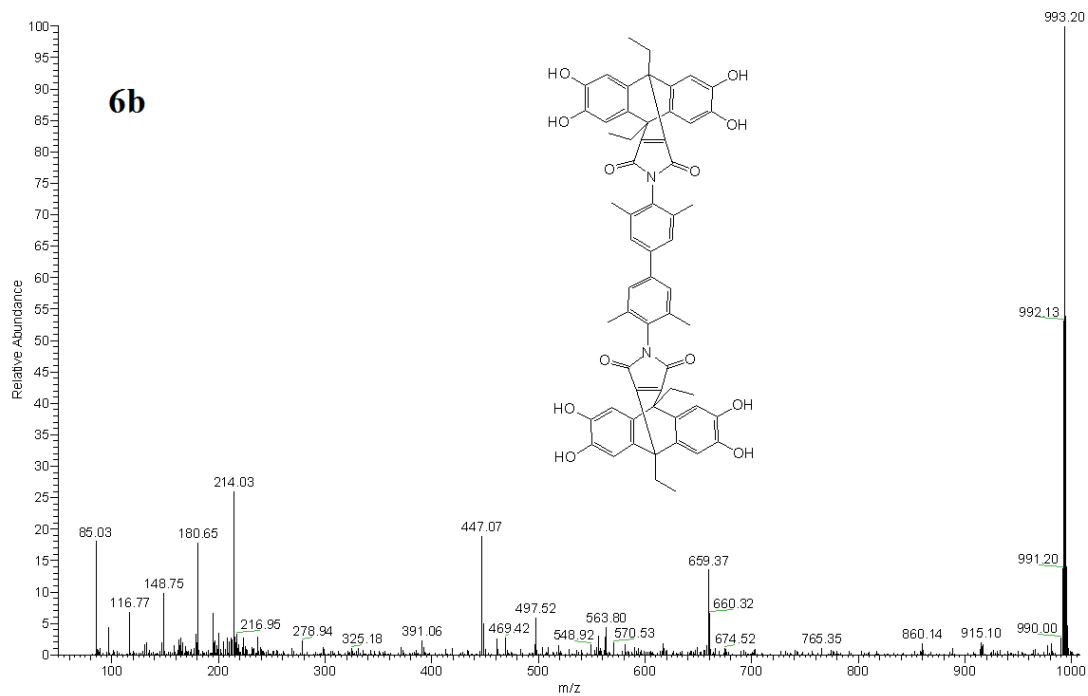
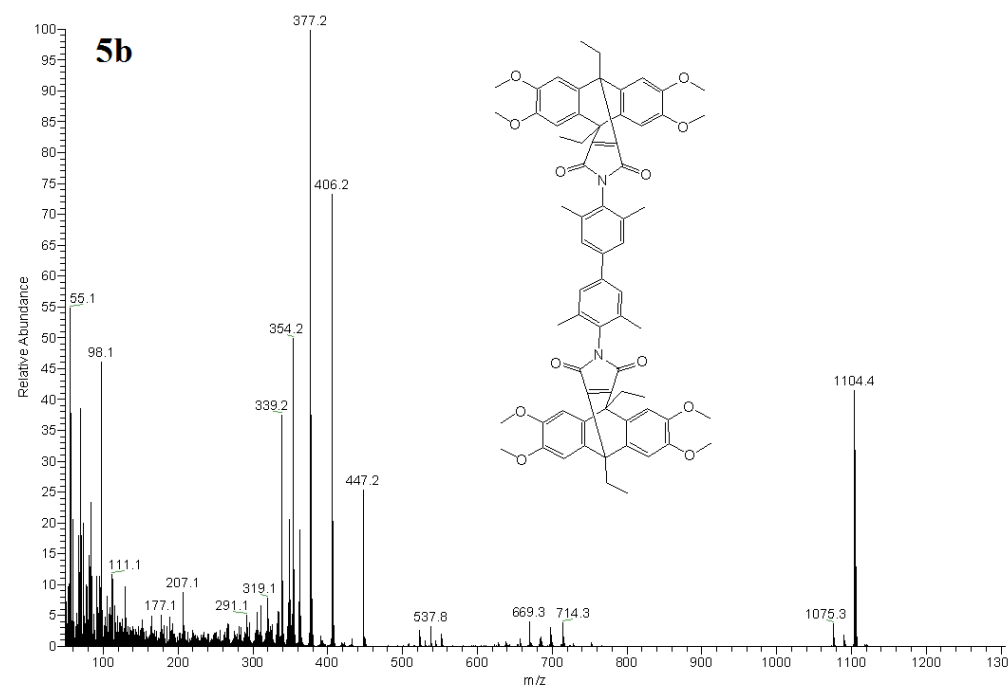


Figure S2k: : Typical mass Spectrum of 5b & 6b

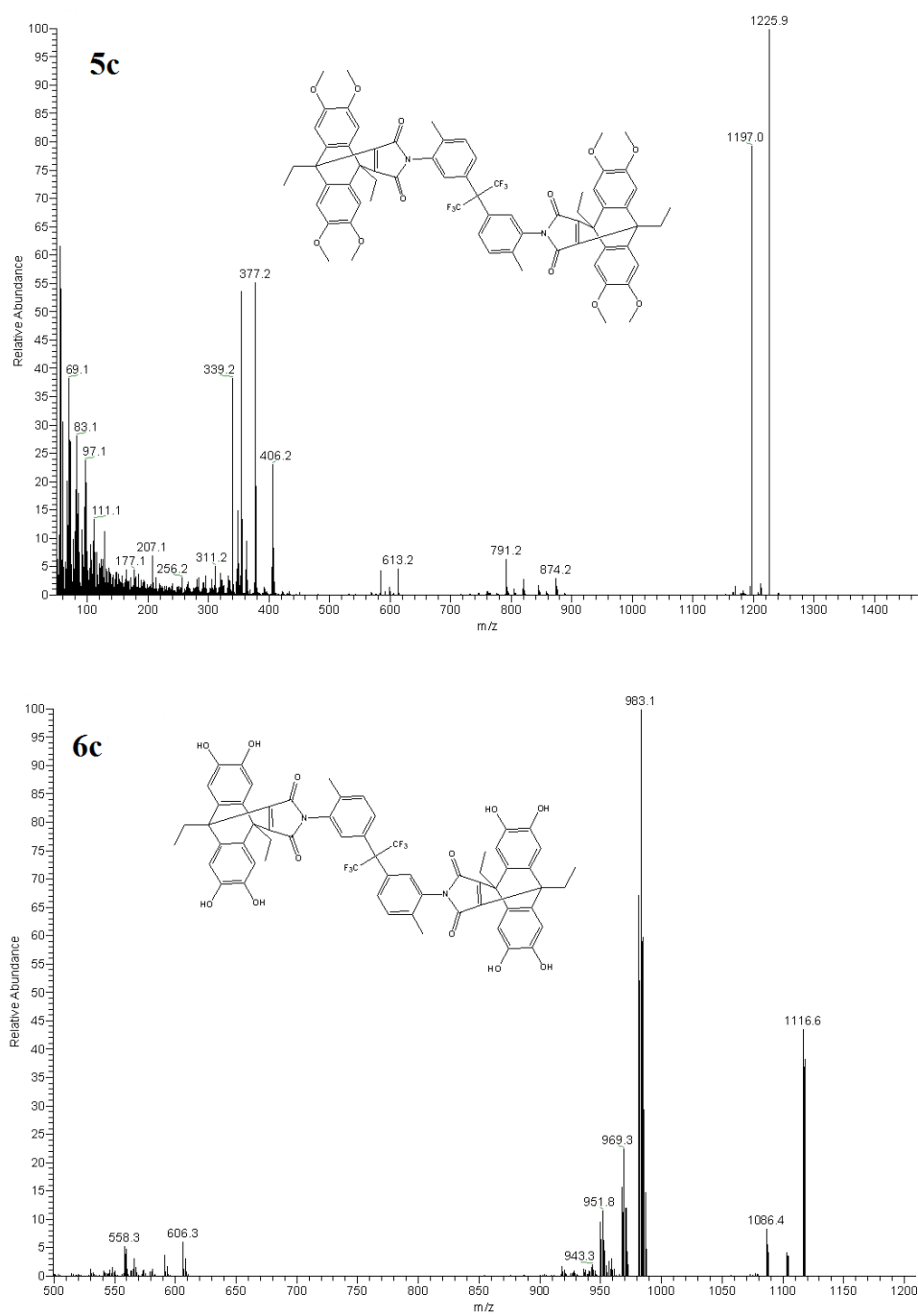


Figure S2l: Typical mass Spectrum of 5c & 6c

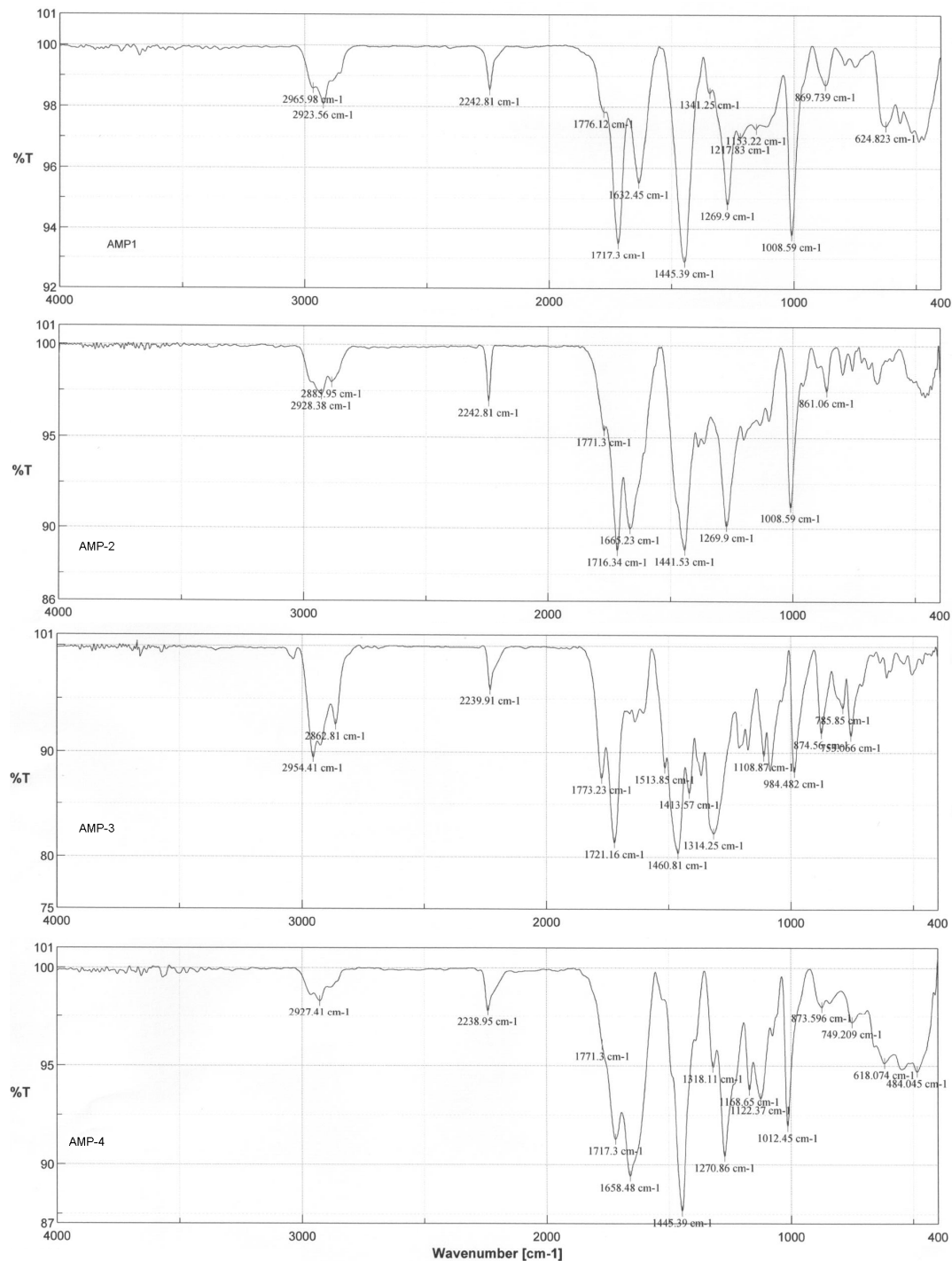


Figure S3: FTIR Spectrum of AMPs (1-4): Discussion pertaining to the IR spectral relationships between the polymers and starting precursors and monomers offers a good support for the proposed structure of all PIM-Rs. The peaks labeled (between 1716-1776) correspond to the imide links. The peak around 2236-2242 is characteristic of nitrile group. Moreover it is clear from the spectrum that the base catalysed polymerisation condition does not affect the imide linkage as supported by bands.

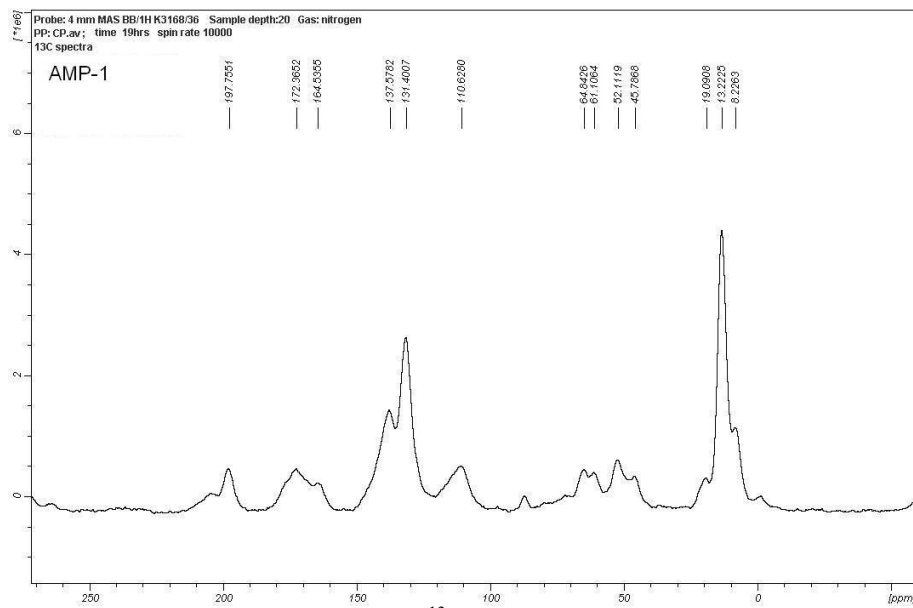


Figure S4a : Solid state ¹³C NMR spectrum of AMP-1

The solid state ¹³C NMR (600 MHz) spectrum of AMP-1 was examined and the signal positions were located precisely with the help of solution as well as solid state ¹³C NMR spectra of monomer (6a) and precursor molecules. The signals at 8.2 and 13.2 (belong to spiroanthracenes unit) represent two type of methyl groups of the proposed repeat unit. The signal at 19 corresponding to methylene groups of the spiroanthracenes unit. Two quaternary carbons come under signals at 61-64 as and 134. The overlapped signals between 110 and 197 representing aromatic carbons within the repeat unit. Based on the information retrieved from ¹³C NMR spectra of the precursor molecules, the overlapping resonances can be confidently assigned different carbon environments.

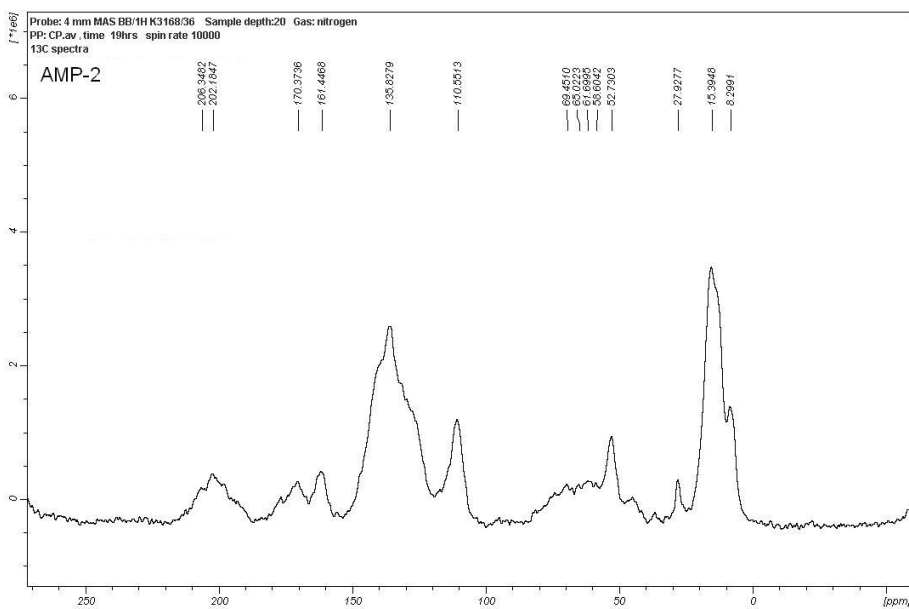
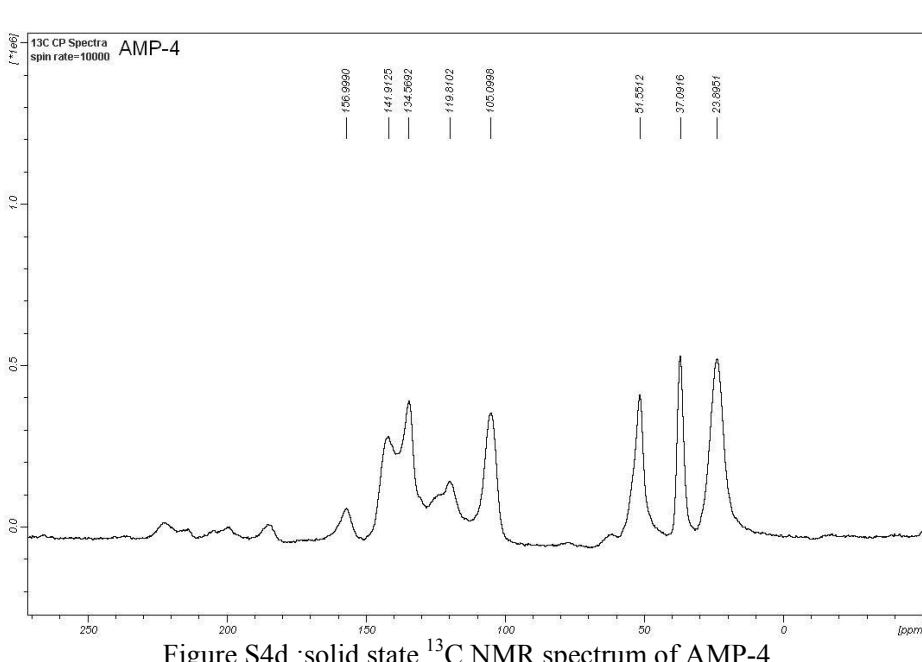
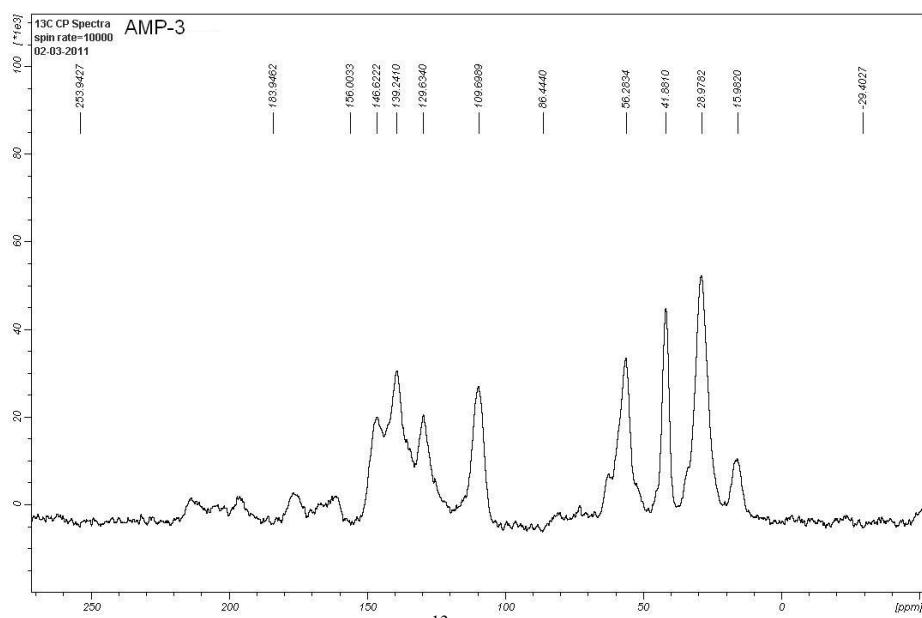


Figure S4b : Solid state ¹³C NMR spectrum of AMP-2



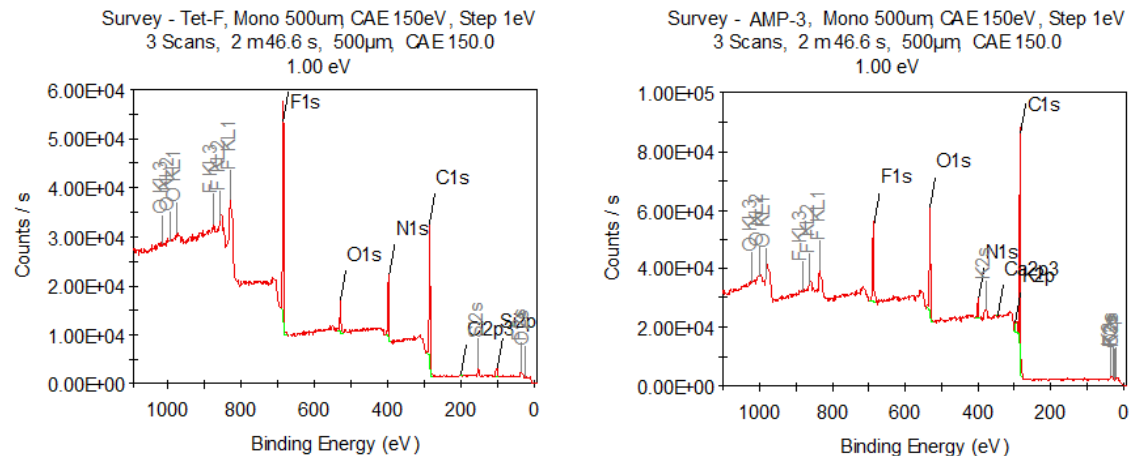


Figure S5. XPS survey spectrum of tetrafluoroterephthalonitrile (monomer) and AMP-3

X-ray photoelectron spectroscopy is an additional technique which was used for the elemental analysis except Hydrogen. The XPS survey of monomer tetrafluoroterephthalonitrile and **AMP-3** reveals the presence of carbon, nitrogen, oxygen and fluorine. The binding energy of the F1s at 685-687.97 eV confirms the presence of fluorine in both monomer and **AMP-3**. The fluorine analysis of **AMP-3** shows only a trace amount compared to monomer. This can be considered as the F atoms present in the repeat units of AMP-3 and consequently confirm the proposed network structure of AMP3.

XPS-Tet-F					
Name	Peak BE	Height Counts	FWHM eV	At. %	Q
F1s	685.2	6081	2.1	22.4	1
C1s	284.6	2588	2.7	57.37	1
N1s	397	1187	2.13	10.34	1
O1s	529.1	692.1	2.69	5.71	1
Si2p	98.92	193.6	2.5	3.88	1
Cl2p	198.1	35.97	2.99	0.3	1

XPS-AMP-3					
Name	Peak BE	Height Counts	FWHM eV	At. %	Q
F1s	687.2	1311	2.65	4.56	1
C1s	284.6	5987	2.2	72.93	1
N1s	399.9	579.3	1.99	2.91	1
O1s	532.2	2493	3.77	17.89	1
K2p	293.5	332	4.04	1.38	1
Ca2p	347.6	93.27	2.72	0.33	1

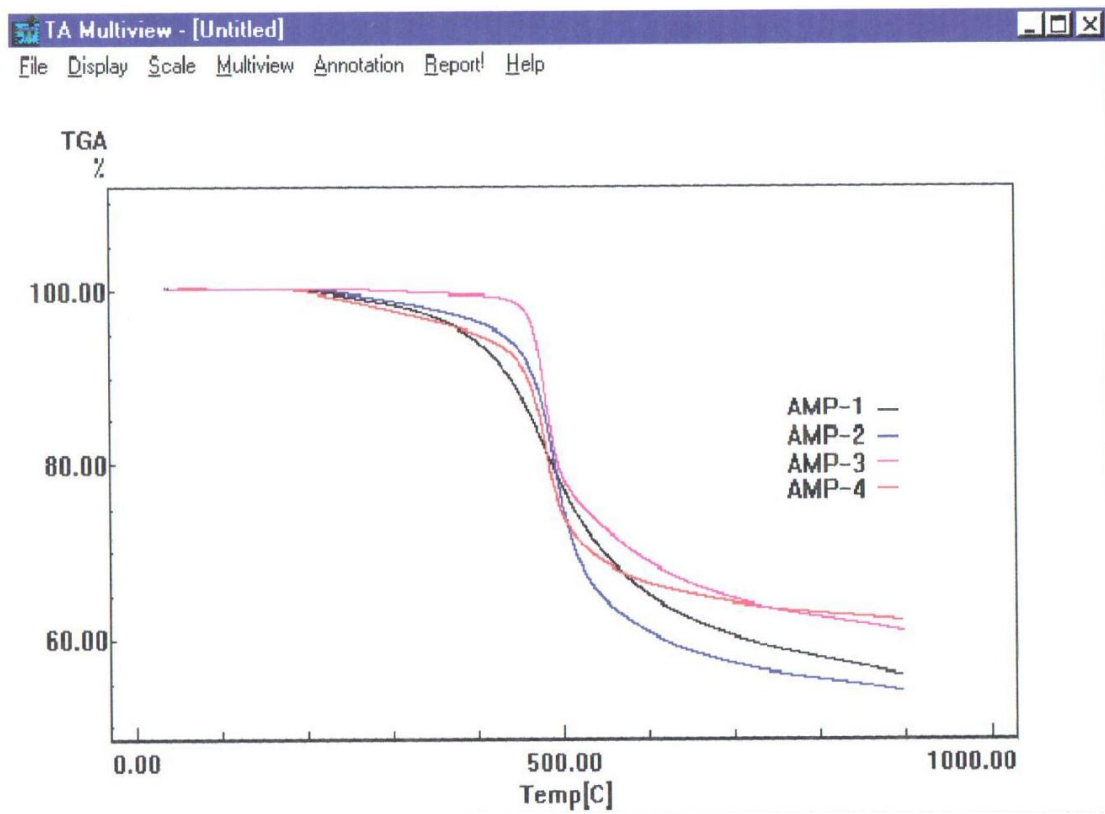


Figure S6. Thermogravimetric traces of AMPs (1-4). Samples were run under nitrogen atmosphere with a heating rate of 10 °C.

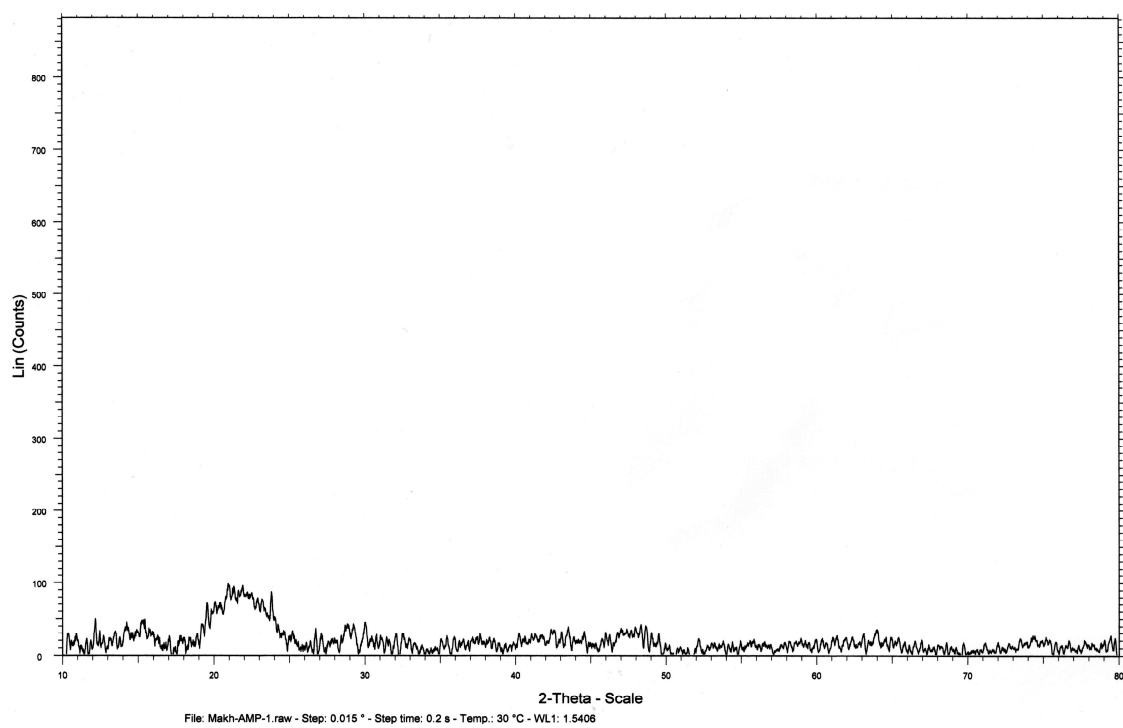


Figure S7a. The powder XRD diffraction pattern of AMP-1

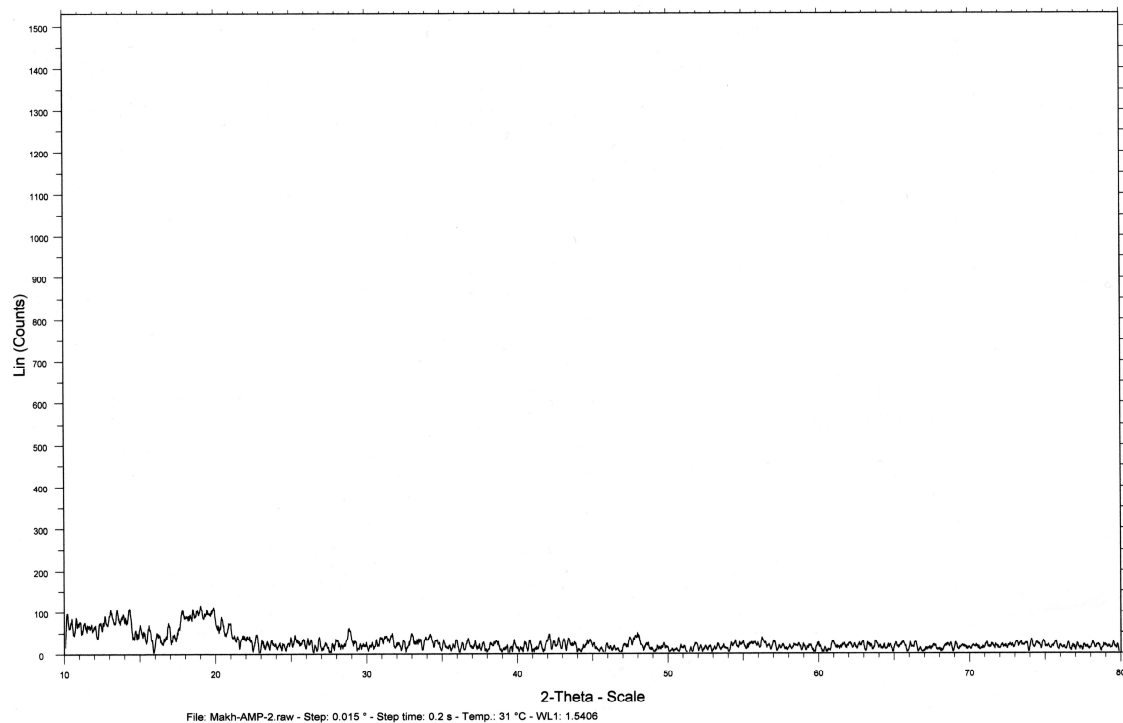


Figure S7b. The powder XRD diffraction pattern of AMP-2

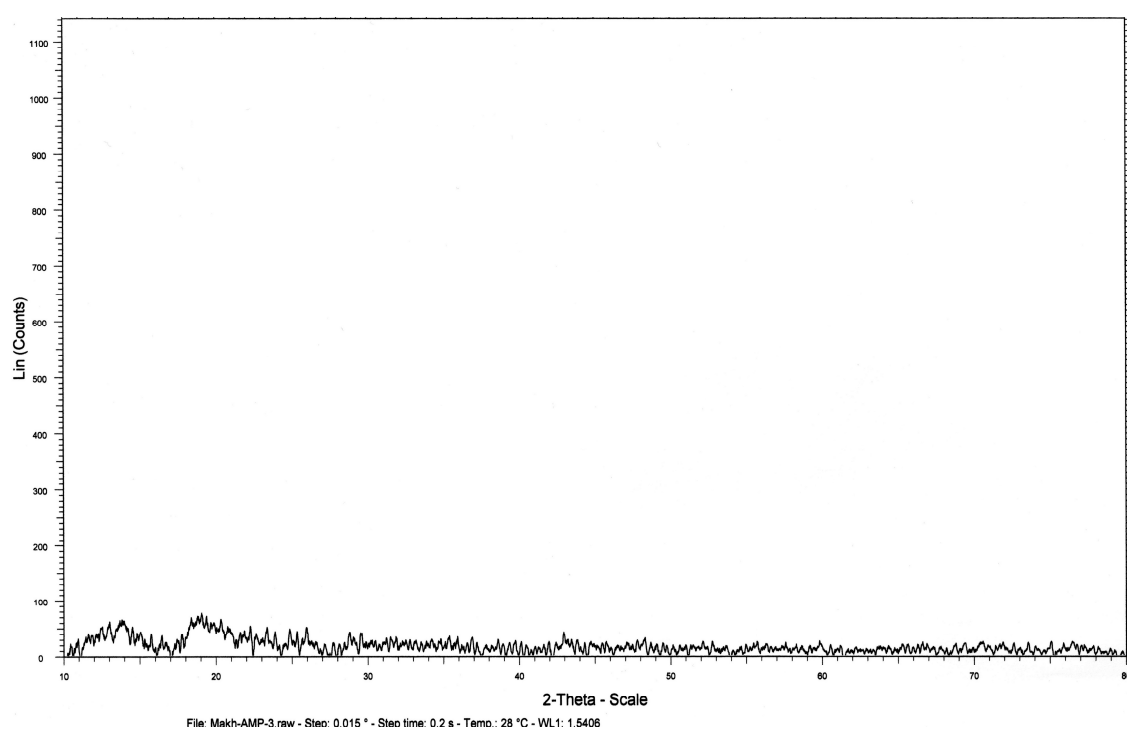


Figure S7c. The powder XRD diffraction pattern of AMP-3

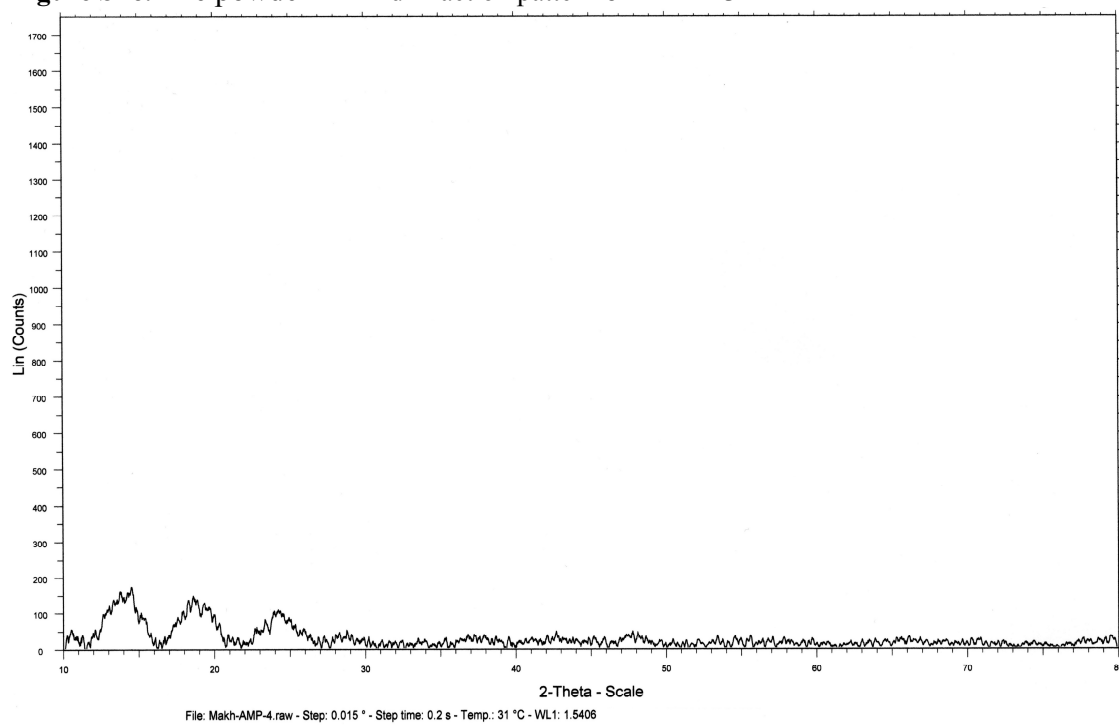


Figure S7d. The powder XRD diffraction pattern of AMP-4

The absence of sharp diffraction pattern indicate that the prepared AMPS are not crystalline.

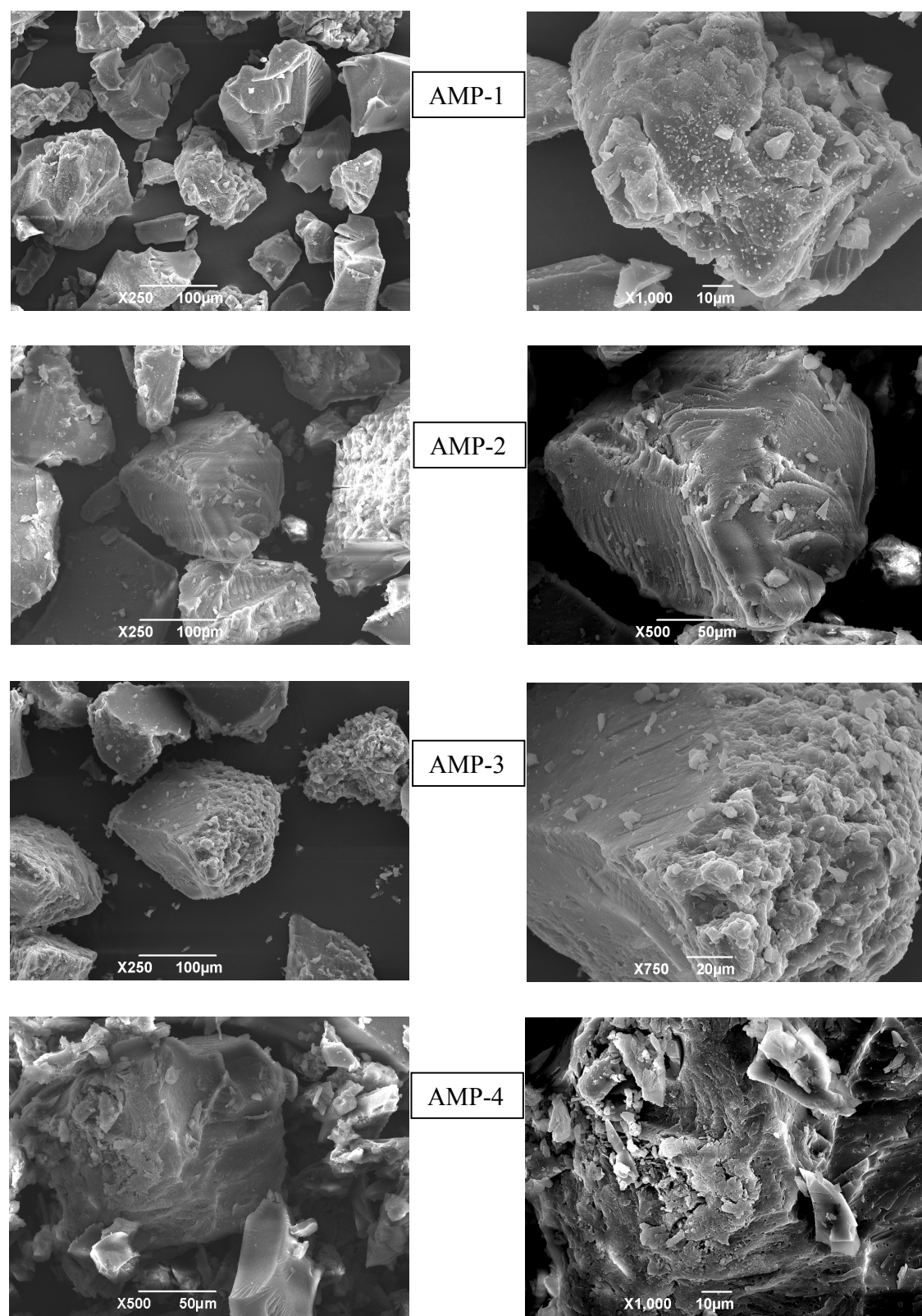


Figure S8. SEM images for AMPs.

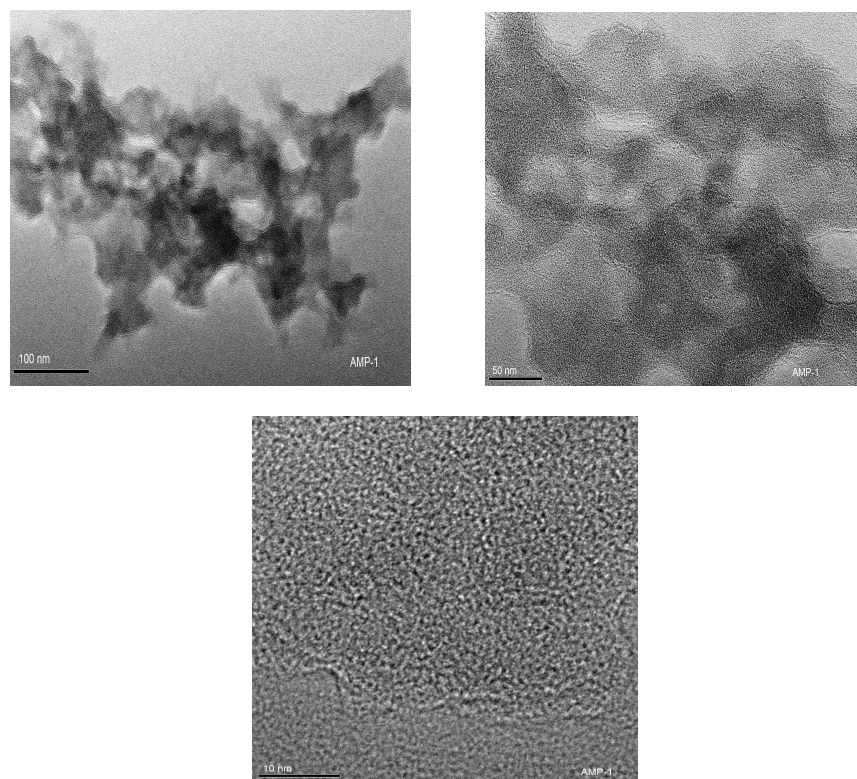


Figure S9a. HRTEM images of AMP-1

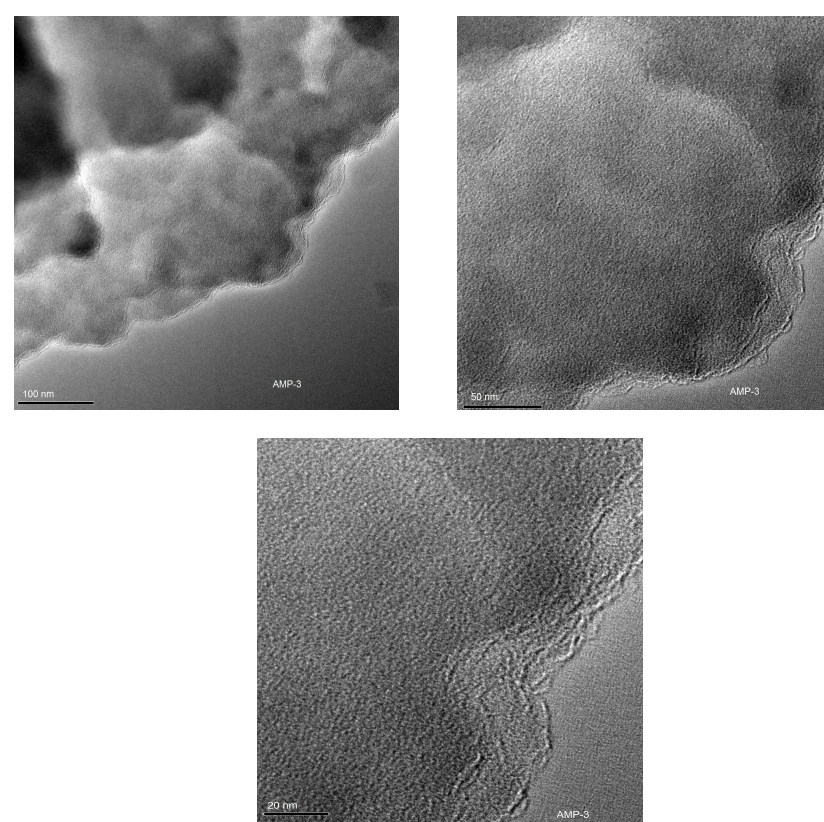


Figure S9b. HRTEM images of AMP-3

HRTEM images of AMP-3 illustrates its microporosity (Wormhole like structure) and structural stability under the experimental condition (300 kV). The pore dimensions are in good agreement with the micropore size distribution as calculated by the H-K and NLDFT methods.

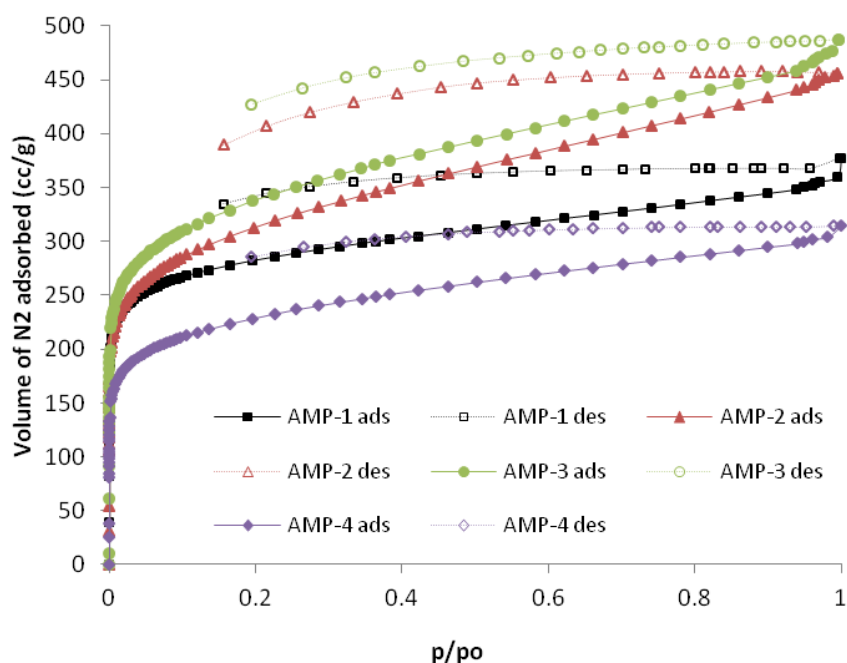


Figure S10a. N₂ sorption isotherms for AMPs (1-4) at 77 K. The filled markers are adsorption points and open markers are desorption.

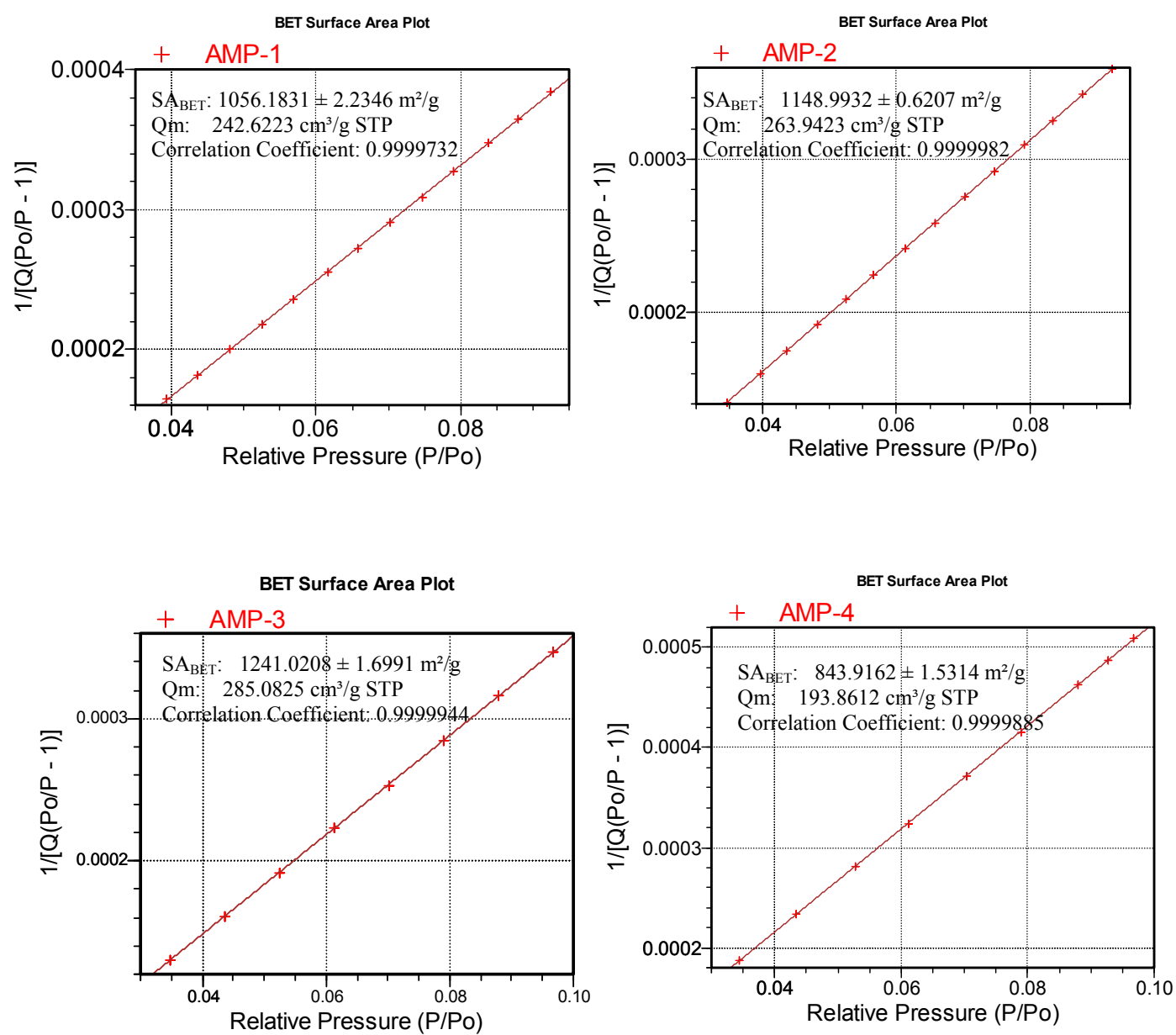


Figure S10b. BET plots for AMP (1-4); pressure ranges: $P/P_0 = 0.030$ to 0.10 at 77 K. The correlation coefficient is indicated.

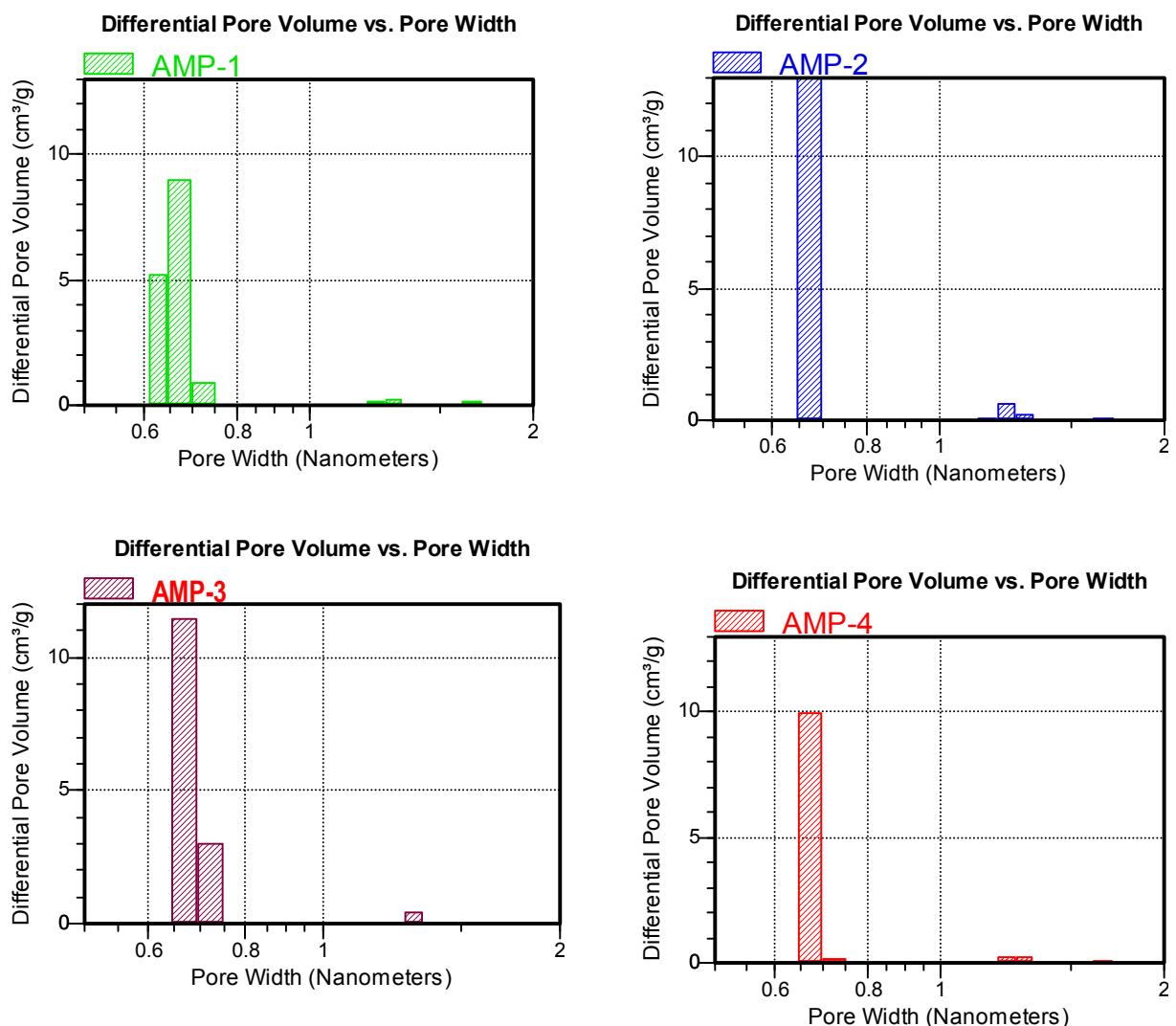


Figure S11a. The Pore Size Distribution of AMPs was calculated from the N₂ adsorption isotherm at 77 K by the Non-Local Density Functional Theory (NLDFT) method. All the plots show a high population of sub-nanometer micropores

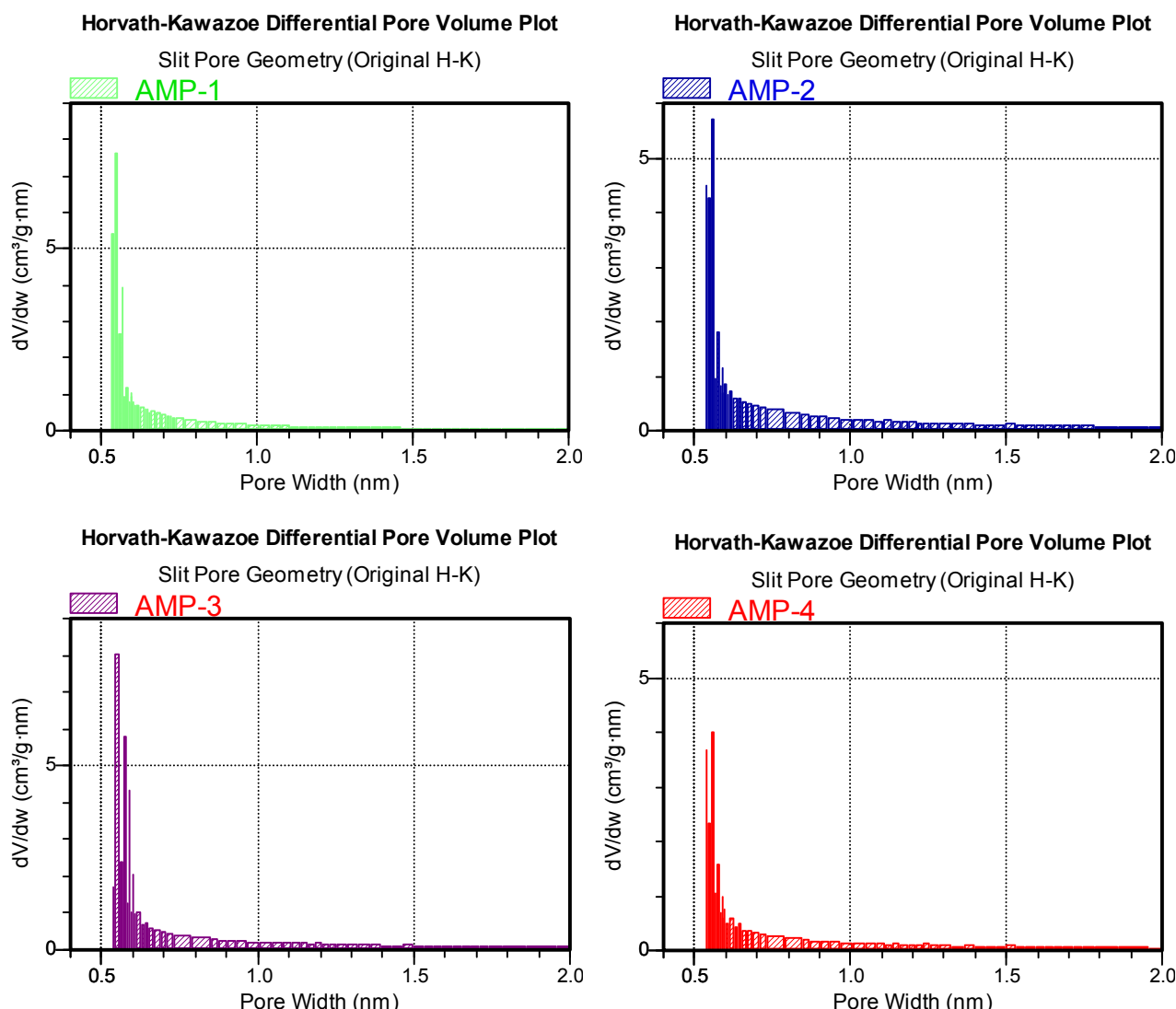


Figure S11b. The Pore Size Distribution of AMPs was calculated from the N_2 adsorption isotherm at 77 K by the Horvath- Kawazoe (HK) method. All the plots show a high population of sub- nanometer micropores.

The micropore distributions obtained from the HK and NLDFT methods are quite similar. A single narrow sharp peak on each of the pore size distribution curves for the samples under study indicates that the AMPs have mono-disperse pores, with diameters less than 1 nm.

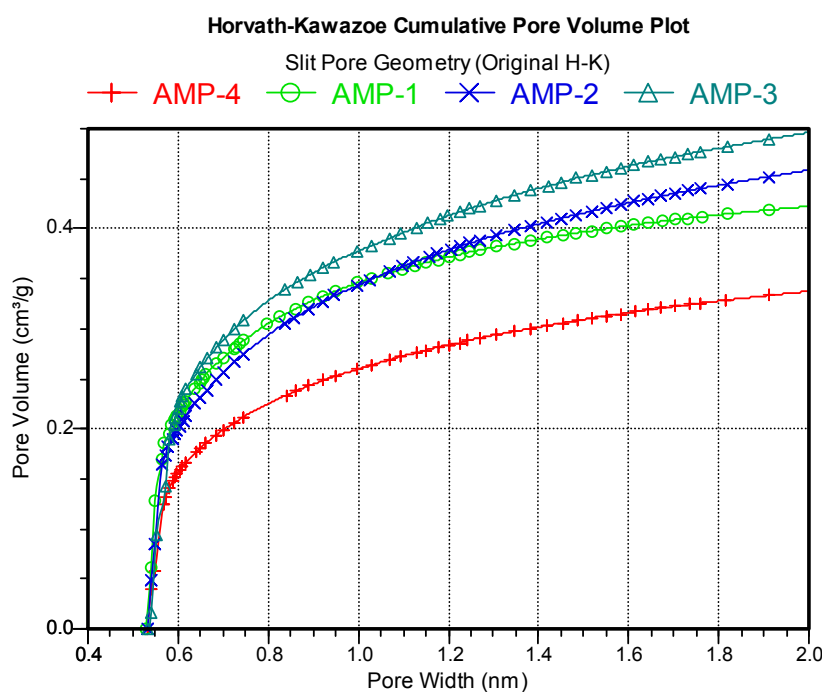


Figure S12. HK Cumulative pore volume plot
Cumulative Pore Volume vs. Pore Width

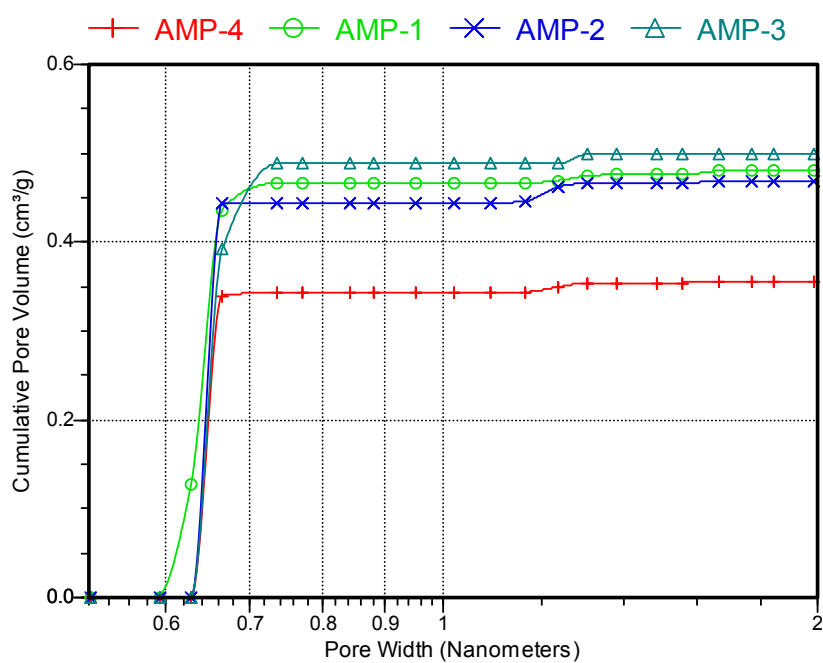


Figure S13. NLDFT Cumulative pore volume plot

Both HK and NLDFT cumulative pore volume plots explore the pore size vs pore volume pattern. Both calculations show the similarity in the pore pattern especially homogeneity in pore sizes.

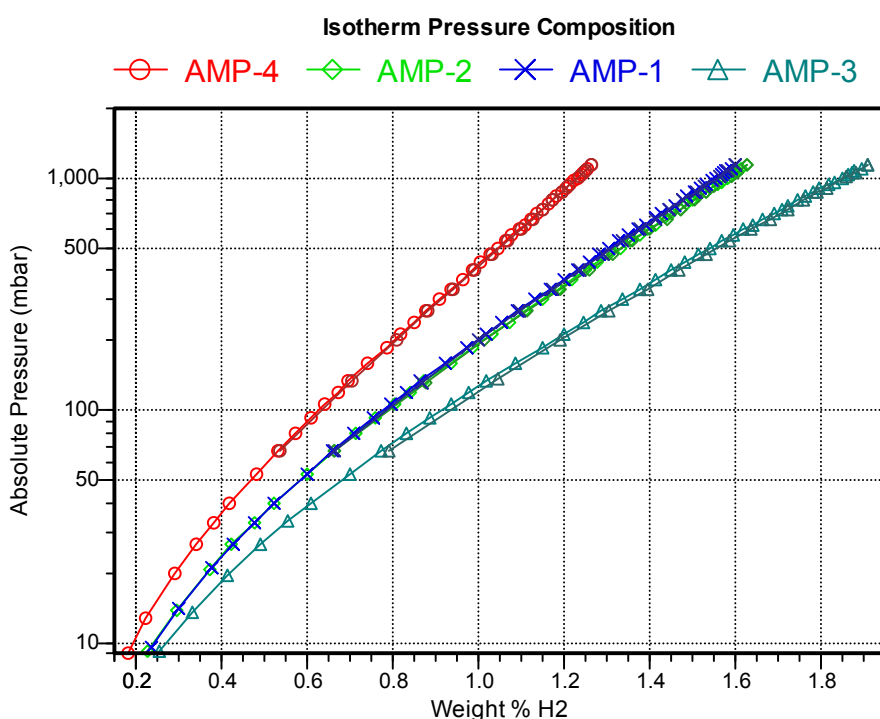


Figure S14a. H₂ uptake of AMPs (1-4) at 77 K

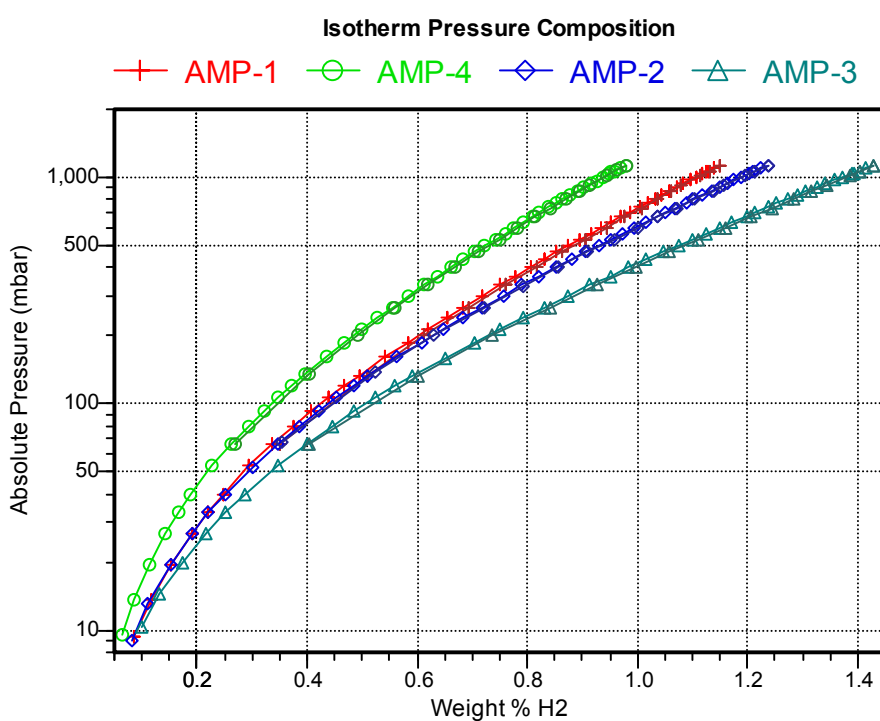


Figure S14b. H₂ uptake of AMPs (1-4) at 87 K

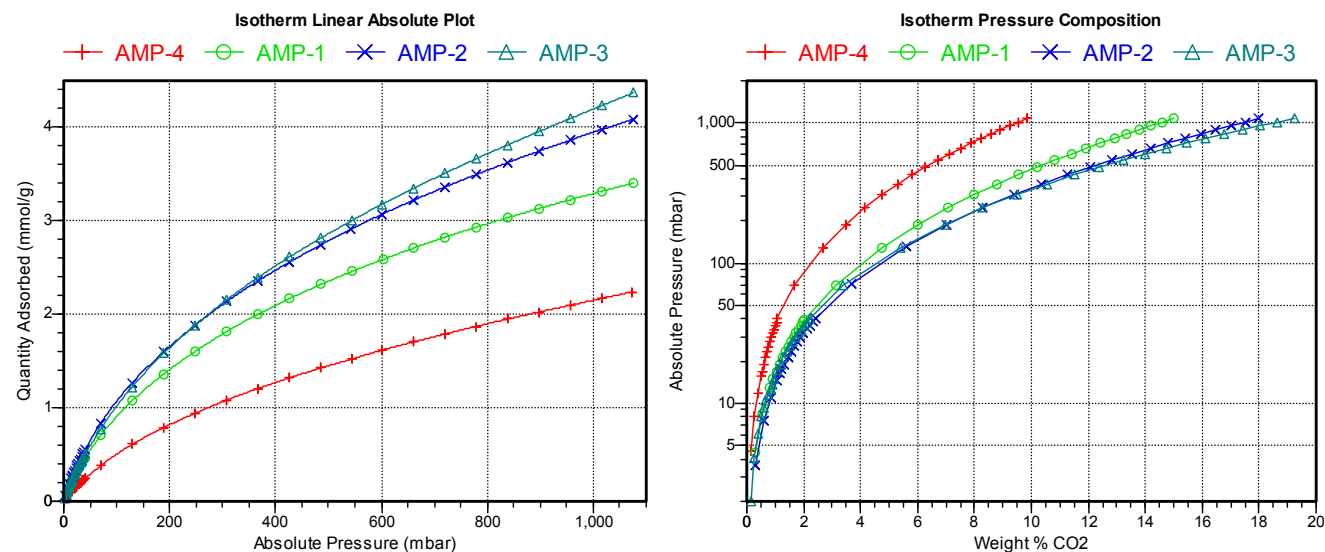


Figure S15a. CO₂ uptake of AMPs (1-4) at 273 K

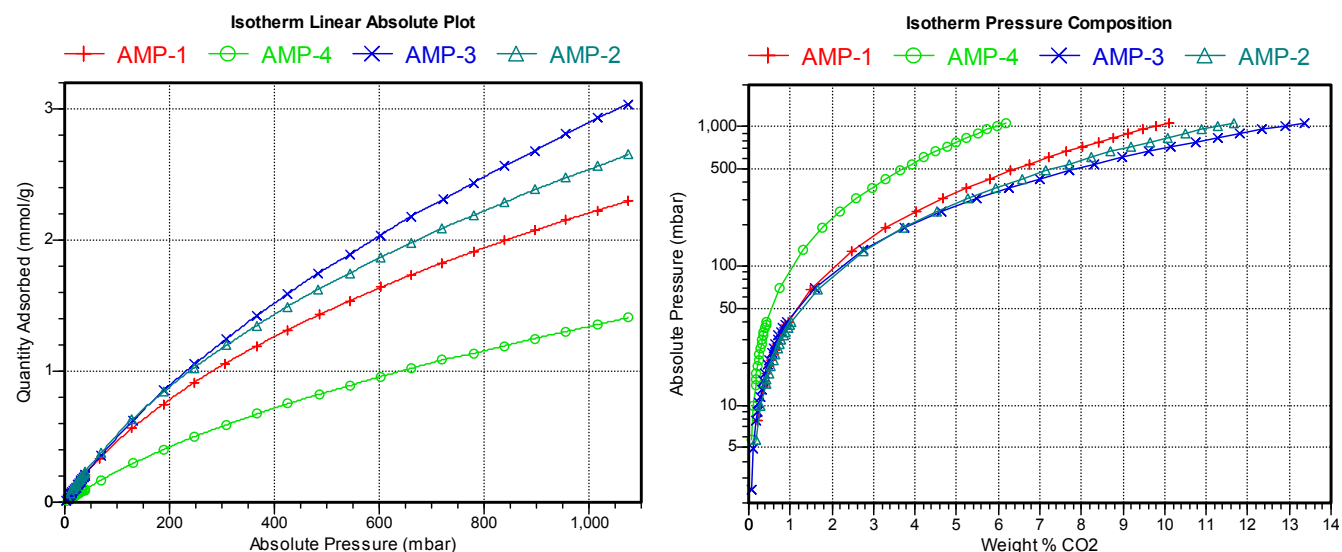


Figure S15b. CO₂ uptake of AMPs (1-4) at 295 K

High pressure volumetric CO₂ adsorption

The quantity of carbon dioxide adsorbed by AMPs was estimated by HPVA-100 particulate system capable of achieving pressures up to 100 bar. The high precision, high pressure transducer provides a reading accuracy of $\pm 0.04\%$ full scale with a stability of $\pm 0.1\%$. About 0.5 g of sample is placed in a clean steel sample cell. A gasket made of stainless steel is placed on the cell top to prevent materials from being sucked into the HPVA system and connected to the degas station and degassed at 120 °C using a furnace till the vacuum gauge reads below 0.6 milli Torr. The degassed sample cell then connected to analysis port and run the adsorption experiment at 295 K. The operating valves automatically open and allow CO₂ gas into the sample cell, and its pressure and temperature were automatically measured (see Fig. 16). The adsorption/desorption isotherms are typically analyzed up to 40 bar at near ambient temperatures due to CO₂ condensation at higher pressures.



HPVA II – High Pressure Volumetric Analyser (HPVA 100)

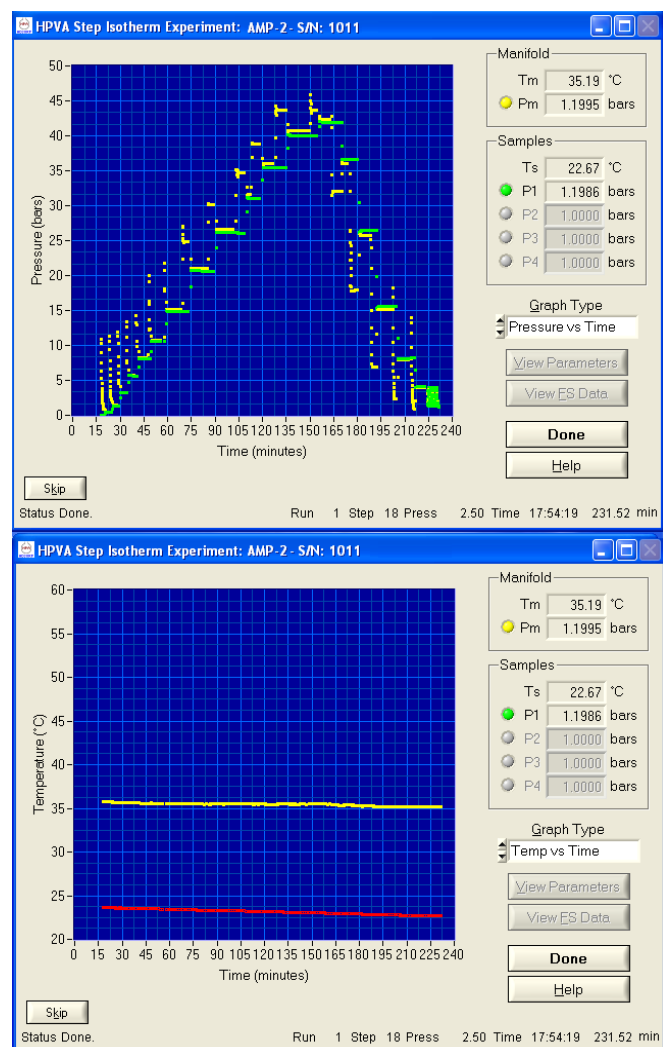


Figure S16. Typical step isotherm and temperature plots vs time

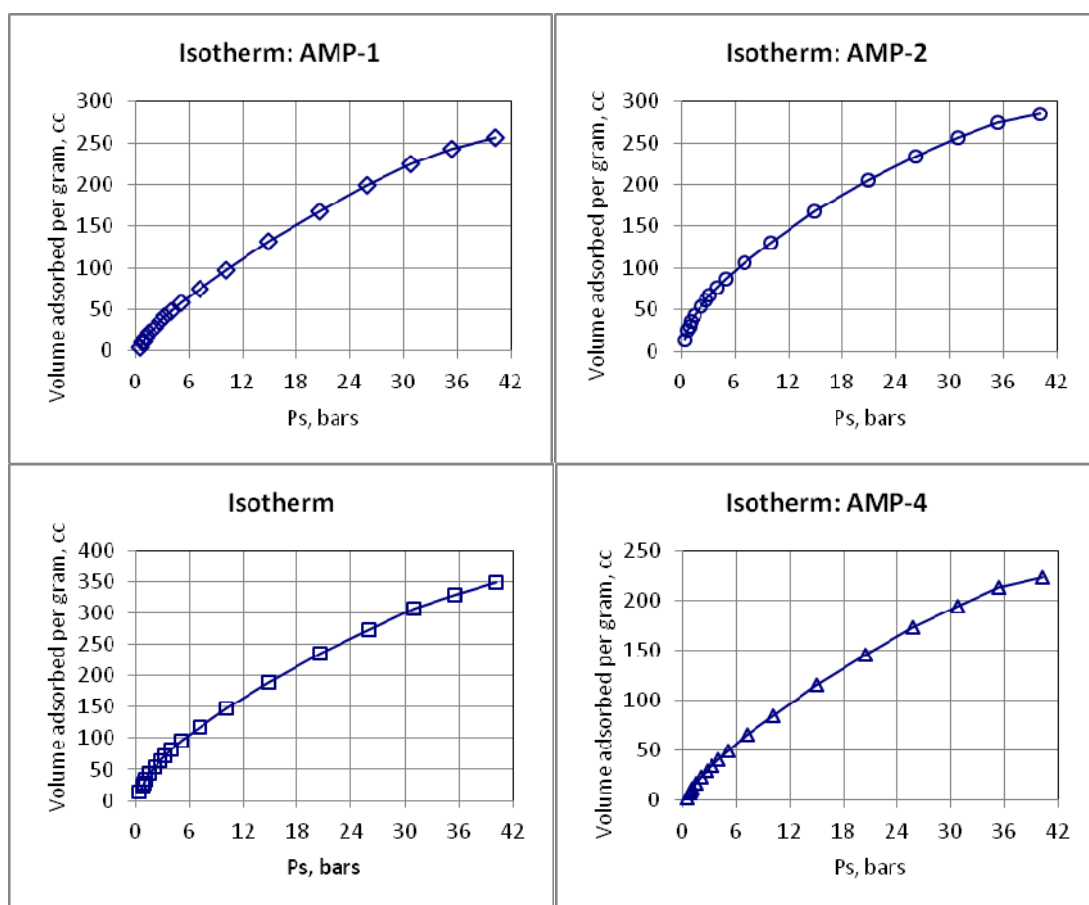


Figure S17. High pressure volumetric CO₂ uptake results for AMPs at 295 K